Integrating human behaviour and building vulnerability for the assessment and mitigation of seismic risk in historic centres: Proposal of a holistic human-centred simulation-based approach

Manuscript Details

Manuscript number	IJDRR_2019_499_R2
Title	Integrating human behaviour and building vulnerability for the assessment and mitigation of seismic risk in historic centres: Proposal of a holistic human-centred simulation-based approach
Article type	Research Paper

Abstract

The complexity of historic centres implies that risk assessment in those areas should be based on joint analyses of the characteristics of the built environment and the population's features, exposure and interaction with the surrounding environment. Such a holistic approach is urgently needed to evaluate the impact of mitigation strategies, especially in sudden onset disasters, and, mainly, earthquakes. In fact, the effectiveness of retrofitting interventions and emergency management strategies on the safety level depends greatly on such interactions, also in relation to the path network features. This work proposes a PDCA-based methodology for earthquake risk assessment which innovatively combines built environment damage assessment with a simulation of human evacuation behaviour so as to identify potentially inaccessible evacuation paths and urban areas, define related paths/areas safety levels and evaluate the impact of proposed retrofitting and management strategies on the population's safety in an emergency. To this end, a validated seismic vulnerability index method for masonry façade walls is combined with empirical damage assessment correlations (debris depth estimation in outdoor spaces) to create post-earthquake damage scenarios. Then, these are used as input data for evacuation process assessment through an existing earthquake pedestrians' evacuation simulator. Paths and safe areas risk indices are proposed to evaluate the main behavioural issues in emergency conditions. Finally, different solutions aimed at improving evacuation safety (i.e. emergency plans, rescuers' access strategies and retrofitting of buildings) are proposed and discussed for a significant case study, the historic centre of Coimbra, Portugal.

Keywords	human factor in risk assessment; earthquake; emergency evacuation; evacuation simulation; human behaviour in emergency; historic urban environment

Corresponding Author	Tiago Ferreira
Corresponding Author's Institution	University of Minho
Order of Authors	Aleksandar Zlateski, Michele Lucesoli, Gabriele Bernardini, Tiago Ferreira

POSTPRINT OF: Zlateski A, Lucesoli M, Bernardini G, Ferreira TM (2020) Integrating human behaviour and building vulnerability for the assessment and mitigation of seismic risk in historic centres: Proposal of a holistic human-centred simulation-based approach. International Journal of Disaster Risk Reduction 43:101392. https://doi.org/10.1016/j.ijdrr.2019.101392

POSTPRINT OF: Zlateski A, Lucesoli M, Bernardini G, Ferreira TM (2020) Integrating human behaviour and building vulnerability for the assessment and mitigation of seismic risk in historic centres: Proposal of a holistic human-centred simulation-based approach. International Journal of Disaster Risk Reduction 43:101392. https://doi.org/10.1016/j.ijdrr.2019.101392

Integrating human behaviour and building vulnerability for the assessment and mitigation of seismic risk in historic centres: Proposal of a holistic human-centred simulation-based approach

Highlights

- Earthquake risk in historic urban environment is investigated.
- A simulation-based approach is offered for risks analysis/mitigation strategies proposal.
- A case study application is used to demonstrate the method capabilities.
- Simulations focus on the evacuation process to assess the population's safety.
- Mitigation strategies on building retrofit and evacuation plan are validated through simulations.

Integrating human behaviour and building vulnerability for the assessment and mitigation of seismic risk in historic centres: Proposal of a holistic human-centred simulation-based approach

Abstract

The complexity of historic centres implies that risk assessment in those areas should be based on joint analyses of the characteristics of the built environment and the population's features, exposure and interaction with the surrounding environment. Such a holistic approach is urgently needed to evaluate the impact of mitigation strategies, especially in sudden onset disasters, and, mainly, earthquakes. In fact, the effectiveness of retrofitting interventions and emergency management strategies on the safety level depends greatly on such interactions, also in relation to the path network features. This work proposes a PDCA-based methodology for earthquake risk assessment which innovatively combines built environment damage assessment with a simulation of human evacuation behaviour so as to identify potentially inaccessible evacuation paths and urban areas, define related paths/areas safety levels and evaluate the impact of proposed retrofitting and management strategies on the population's safety in an emergency. To this end, a validated seismic vulnerability index method for masonry façade walls is combined with empirical damage assessment correlations (debris depth estimation in outdoor spaces) to create post-earthquake damage scenarios. Then, these are used as input data for evacuation process assessment through an existing earthquake pedestrians' evacuation simulator. Paths and safe areas risk indices are proposed to evaluate the main behavioural issues in emergency conditions. Finally, different solutions aimed at improving evacuation safety (i.e. emergency plans, rescuers' access strategies and retrofitting of buildings) are proposed and discussed for a significant case study, the historic centre of Coimbra, Portugal.

Keywords: human factor in risk assessment; earthquake; emergency evacuation; evacuation simulation; human behaviour in emergency; historic urban environment

1 Introduction

Facing disaster risks in complex built environments means considering the challenging system of relations between human, physical, organizational and intangible factors so as to move towards a better risk assessment and an improved safety design and operation in emergency conditions (Francini et al. 2018; Shrestha et al. 2018; French et al. 2018).

From this point of view, urban built environments located in natural hazard-prone areas are a paramount scenario for such interactions, while dealing with possible risk assessment and proposals for safety-increasing solutions to be adopted and also supported by public bodies (Moore 2008; Lämmel et al. 2010; Ferreira et al. 2016; Cer et al. 2017; Shrestha et al. 2018). Historic city centres represent a particularly relevant scenario (D'Amico and Currà 2014; Maio et al. 2018; Quagliarini et al. 2018), especially when considering sudden onset disasters like earthquakes (Gavarini 2001; Comerio 2004; Vicente et al. 2014; Filippova et al. 2018), which have the potential to trigger critical situations, mainly during the initial phases of disaster aftermath, i.e. evacuation and rescuers' access to damaged areas (Hubbard et al. 2014; Santarelli et al. 2018b; Dolce et al. 2018; Aguado et al. 2018). Moreover, possible earthquake-induced damage to urban paths is affected by both the vulnerability of the building stock (Ferreira et al. 2014; Lagomarsino & Giovinazzi 2006; Ortiz & Ortiz 2016; Santarelli et al. 2018) and the severity of the seismic event (described in terms of magnitude or intensity), and influenced by general and local hazard conditions (Pace et al. 2008; Ismail-Zadeh et al. 2017).

Human safety in complex and compact spaces, like historic urban fabrics, is also heavily influenced by related damage levels (Villagra et al. 2014; Dolce et al. 2018). In particular, the process of evacuating the population along the urban path network could be hindered by

damage preventing people reaching safe areas and trapping them in dangerous ones, and also limiting the effectiveness of the emergency management plan by first responders (Hirokawa and Osaragi 2016; Santarelli et al. 2018b; Robat Mili et al. 2018; Aguado et al. 2018). The combination of vulnerability-reduction interventions on buildings, i.e. seismic retrofitting actions (Egbelakin et al. 2011; Ferreira et al. 2017b; Filippova et al. 2018), and emergency management strategies (Tai et al. 2010; Italian Technical Commission for Seismic Micro-zoning 2014; Robat Mili et al. 2018; Dolce et al. 2018) can improve safety levels in the urban fabric.

The definition of effective risk-mitigation strategies should be supported by analysis of the conditions of disaster scenarios by adopting a performance-based and holistic standpoint, which has to actively consider human behaviour-related aspects (Barbat et al. 2010; Robat Mili et al. 2018; Quagliarini et al. 2018; Dong et al. 2018). To this end, four fundamental pillars should be considered:

(i) The seismic vulnerability assessment of the building stock (Ferreira et al. 2015; Aguado et al. 2018). Mainly resorting to qualitative information (Lagomarsino and Giovinazzi 2006; Lombardo and Cicero 2015), which can be collected through external or remote surveys, empirical methodologies can provide individual vulnerability indicators (Ferreira et al. 2014; Ferreira et al. 2017a; Santarelli et al. 2018a).

(ii) The prediction of post-earthquake damage scenarios through the correlation between seismic severity and building vulnerability (Lagomarsino and Giovinazzi 2006; Santarelli et al. 2018a). Empirical-based methods can be further used to estimate post-earthquake damage scenarios for different levels of seismic severity (Ferreira et al. 2017a). In respect to urban fabric conditions in the immediate aftermath, the deposition of debris along streets is a key element in terms of evacuation. Such material, which largely results from the out-of-plane collapse of façade walls (Aguado et al. 2018), can severely compromise the evacuation

conditions by blocking the urban paths. Previous methods have tried to address this issue by using simple geometrical approaches or joint vulnerability–earthquake severity methods (Anastasiadis and Argyroudis 2007; Italian Technical Commission for Seismic Micro-zoning 2014; Zanini et al. 2017; Santarelli et al. 2018a).

(iii) The representation of the earthquake evacuation process by including post-earthquake scenario conditions and by focusing on the pedestrians' evacuation process (Dilley et al. 2005; Hirokawa and Osaragi 2016; Bernardini et al. 2016; Kimms and Maiwald 2018). In general terms, many of the approaches to evacuation simulation in outdoor urban spaces are essentially based on simulation models developed for indoor conditions (e.g. fire) or general purpose evacuation (Bernardini et al. 2016). Hence, the results are affected by the effective modelling of the numbers of individuals involved and their earthquake-related behaviours and interactions with debris/damage and the state of the path and urban spaces (Lu, Yang, Cimellaro, & Xu 2019). Macroscopic models are generally avoided because of the lack of specific earthquake-evacuation databases to define hydrodynamics motion rules. Microscopic models (Parisi and Dorso 2005) are often preferable since they consider behavioural aspects associated with each individual, as well as with the specific interactions between evacuees and the earthquake-modified urban scenario (Hashemi and Alesheikh 2013; D'Orazio et al. 2014; Bernardini et al. 2016; Oki and Osaragi 2017; Lu et al. 2019). Cellular automata models offer computational simplicity and efficiency, but they are mainly used for indoor evacuation purposes (Song, Xie, & Su 2019), by combining the model with simulation platforms such as SIMULEX (Thompson and Marchant 1995) or others (Chu et al. 2019). Modifications to the Social Force model have been provided in many works to represent the evacuation process in outdoor urban spaces from a microscopic point of view (Bernardini et al. 2016; Lu et al. 2019). Other models combine multiagent-based/Agent Based Model (ABM)-based tools with previous motion equations so as to include earthquake-related

desires and choices in individuals' evacuation (Yu et al. 2018). The main urban spaces applications take advantage of consolidated simulation platforms (e.g. RoboCup (Okaya and Takahashi 2015)) or of the implementation of specific software tools (Bernardini et al. 2016; Lu et al. 2019). From this point of view, the combination of the Social Force Model and Agent Based Model techniques has shown interesting capabilities in describing behaviours like the avoidance of obstacles or interactions with falling debris. Furthermore, preliminary validations on such models were provided by using real-world data (D'Orazio et al. 2014).

(iv) The definition of key performance indicators (KPI) for safety assessment, focused on the population's perspective (O'Brien et al. 2017; Dong et al. 2018). From the occupants' safety standpoint, the safety of the overall evacuation procedure can also be measured by indices specifically developed for the effect, which assess the evacuees' motion conditions (Xiao et al. 2016), including the identification of possible threats (Tai et al. 2010; Bernardini et al. 2016; Robat Mili et al. 2018). Such KPIs can summarize the impact of the adoption of different risk mitigation strategies, based on either building retrofitting or emergency management (Ferreira et al. 2017b), by comparing their value in different scenarios.

Within this framework, the present paper aims at addressing the above issues by proposing an innovative simulation-based methodology focused on the evacuation process. In order to achieve this ambitious goal, an index-based seismic vulnerability assessment method for masonry façade walls is herein applied to create post-earthquake damage scenarios for the historical centre of Coimbra, Portugal, which are then used as input to simulate pedestrians' evacuation in an earthquake. This original procedure, in which building vulnerability and human behaviour are combined, is then used to evaluate the evacuation conditions of the study area, as well as to assess urban criticalities. Different solutions aimed at improving the evacuation conditions, including rescuers' access strategies, are finally proposed and discussed.

2 Methods

This work involves two main methodological phases: (i) the definition of the holistic methodology designed to assess safety levels in evacuation and the proposal and validation of risk-mitigation solutions; and (ii) the application of the methodology developed on a representative case study, with the aim of demonstrating its ability to jointly analyse individuals–environment interactions for different earthquake scenarios.

The proposed holistic methodology is illustrated in Figure 1 according to the Plan-Do-Check-Act (PDCA) cycle methodology, which has been used in previous works for disaster safety and emergency management evaluations (Moore 2008; Bernardini et al. 2016).

In general terms, it takes advantages of a holistic approach to earthquake safety (Vicente et al. 2014; Bernardini et al. 2016), which combines the effects of environmental conditions on the evacuation process, in order to evaluate safety levels in immediate emergency conditions. This involves the analysis of the interactions between individuals and: (i) the urban scenarios, buildings and related earthquake-induced modifications, especially in relation to the evacuation path conditions (e.g. debris from damaged buildings and street network vulnerability); (ii) the emergency management system, including evacuation planning aspects (e.g. locations of assembly areas); and (iii) other individuals.

To jointly combine such aspects, the methodological points identified in Figure 1 are discussed in the following. It is important to highlight that the general framework proposed in Figure 1 can also be used by substituting the proposed specific methods with similar ones. Notations and acronyms used in the following sections are summarised in Appendix A. Literature methods used in this study are included in Appendix B, C and D.

[PLACE HERE FIGURE 1]

2.1 PLAN the actions by creating scenarios for safety assessment analysis

The definition of possible emergency scenarios for historical city centres should involve the *characterization of the physical scenario*. In order to speed up the urban scale application and the definition of different scenarios (Dolce et al. 2018), the use of more expeditious collection, assessment, evaluation and representation approaches is preferable. Data should involve: (i) *urban layout geometry*, including building heights and the configuration of the urban path network, namely through the characterization of the *decision points, network links, assembly areas, access points*, etc. (D'Orazio et al. 2014; Italian Technical Commission for Seismic Micro-zoning 2014; Santarelli et al. 2018b); (ii) *building use,* by considering the presence of highly exposed and strategic buildings (e.g. hospitals, hotels, public administration structures), as well as by characterizing the position and number of inhabitants involved in evacuation; and (iii) *building and urban path network vulnerability*, preferably using simplified assessment techniques. In this work, building vulnerability has been evaluated according to Ferreira et al. (2014) (see Appendix B), whereas urban path vulnerability has been evaluated according to Santarelli et al. (2017) (see Appendix C).

Besides the characterization of the physical scenario, possible emergency scenarios also depend on the *severity of the seismic events* that may occur in the area. Although earthquake severity can be simply described in terms of intensity, this study tries to quantitatively represent this element by forecasting possible building debris on the urban paths in depth terms. The adopted experimental method proposes correlations between seismic magnitude, geometrical building/facing street characterization and building vulnerability (Santarelli et al. 2018a). This method is herein applied to estimate the depth of external debris along urban paths.

Finally, *current evacuation management strategies* in relation to the evacuation plan should be analysed by identifying existing *Codified Safe Areas* (CSA), which are assembly

points, and the rescuers' main access routes (Italian Technical Commission for Seismic Micro-zoning 2014; Zanini et al. 2017). In the cases where there is no evacuation plan, national or international evacuation guidelines can be used.

In this work, the characterization of the *original scenario* refers to the application of such rules to current (pre-intervention) conditions.

2.2 DO by performing evacuation simulation

The evaluation of safety levels for exposed population in immediate aftermath conditions should be performed by adopting validated evacuation simulation models and related software tools (Ronchi et al. 2013; D'Orazio et al. 2014), which should jointly analyse both the *earthquake-induced scenario modifications* and the *evacuation process.*

The *earthquake-induced scenario modifications* should focus on the estimation of debris formation and deposition in the immediate aftermath of an event, to evaluate the eventual availability of post-event evacuation paths.

The *evacuation process* should be evaluated from the analysis of the individuals' actions in earthquake-modified conditions, while seeking help from the rescuers. This can be done by using advanced simulation tools capable of taking advantage of microscopic simulation approaches: these can describe the recurring interactions of individuals with individuals and with environmental elements, while preserving the general holistic approach adopted (Schadschneider et al. 2009; Helbing and Johansson 2010; Thompson et al. 2015; Kuligowski 2016). They can be enriched by including an Agent Based Model-oriented approach (Macal and North 2010), so as to include specific evacuees' behavioural rules in motion simulation, while modelling the surrounding environment as a separate agent and so representing related modifications (building debris formation) rules in the earthquake aftermath (Macal and North 2010; D'Orazio et al. 2014).

A validated Earthquake Pedestrians' Evacuation Simulator (EPES) (D'Orazio et al. 2014), based on the combination between ABM and Social Force Model (SFM) techniques (Helbing and Johansson 2010), is used herein. The simulator, originally proposed for the evacuation analysis of historic centres, is described in detail in Appendix D. According to the ABM approach, the adopted debris depth estimation criteria are solved for each building according to Santarelli et al. (2018)'s methods, which take into account the magnitude of the earthquake, the vulnerability of the analysed building and the geometry of the analysed building/facing street (see Section 2.1.1).

The aim of the individuals' evacuation is to reach an existing CSA. Hence, according to the definition given in Section 2.1.1, the individual's *path* is the union of the *links* used to reach a final node (CSA). As already experimentally noticed, in cases where people are not able to reach a CSA, either because of the surrounding built environment conditions (e.g. blocked paths to a CSA) or due to behavioural issues related to path choice criteria (e.g. social attachment), near pedestrians tend to cluster around the same area by creating a *Spontaneous Assembly Area* (SAA). In practice, these are areas that offer evacuees the best safety and comfort conditions (limited presence of debris, greater distance from damaged buildings, enough space to gather and accommodate people in safety, i.e. in uncrowded conditions). According to group attachment phenomena in the adopted SFM (see Appendix D), the SAA can be indicated as the geometrical centre of the gathering group and by considering all the individuals whose mutual distance is equal to or less than 3 m.

While moving towards a CSA, the individual's choice of evacuation paths can be described as a function of the paths geometry, damage levels and social attachment phenomena (D'Orazio et al. 2014), as given in Appendix D for "spontaneous" conditions[1]. A stochastic error arbitrarily fixed at 10% is considered in this work in order to simulate the

[1] "*Spontaneous*" conditions refer to the human response model according to real-world emergency behaviours.

individual decision of each pedestrian in choosing (or not) a certain path to an assembly area during their movement (Korhonen and Hostikka 2010; Lämmel et al. 2010).

Each input scenario is defined according to data retrieved from Section 2.1.1. In each scenario, it is considered that (Hashemi and Alesheikh 2013; D'Orazio et al. 2014; Hirokawa and Osaragi 2016; Xiao et al. 2016; Bernardini et al. 2016):

- all the individuals hosted by buildings can perform the evacuation process;
- the movement process is performed after the earthquake tremor (they do not move during the earthquake tremor, so as to avoid human body instability) and by considering no pre-movement time (possibly the most critical condition for the flows of pedestrians along the paths since they all start moving together);
- all the debris are considered as generated at the start of the evacuation;
- each pedestrian starts the evacuation process outside the building in which he/she is initially located and ends in one of these conditions: when he/she reaches a CSA; when he/she decides to spontaneously stop in a SAA; at the end of the simulation time (people remain outside either a SAA or CSA);
- according to previous EPES tool validations, the preferred speed of the individual's movement $v_{pref,i}(t)$ in the SFM is equal to 2.1±0.5 m/s (Gaussian distribution). This value is consistent with previous earthquake evacuation databases (also used for EPES setup and validation) and it is aimed at retrieving "average evacuation behaviours" in terms of movement speeds. Hence, the effects of individuals' age and movement abilities, as well as of surrounding environment conditions (i.e. lighting levels) are not considered in this work (D'Orazio et al. 2014);
- the maximum simulation time can be fixed by considering the time needed to reach a CSA by the farthest individual moving at 1 m/s.

Five simulations are carried out for each scenario and mean output values (and related standard deviations) are considered to highlight possible variations of the simulated pedestrian behaviour due to stochastic errors introduced (Helbing and Johansson 2010; D'Orazio et al. 2014). According to (Schadschneider et al. 2009; D'Orazio et al. 2014), 10% is the maximum allowed difference in the simulation outputs. An HP ProDesk 400 G1 MT workstation (Intel® CoreT2M i-4570 CPU @ 3.20GHz, RAM: 8GB; SO: Windows 7 Professional 64-bit) is used for running the simulation.

2.3 CHECK the safety levels by analysing simulation results

The quantitative analysis of the evacuation simulation results is performed through key performance indicators (KPIs). KPIs are essentially based on a human-centric metrics standpoint (O'Brien et al. 2017; Dong et al. 2018) and combine the main factors to evaluate the scenario criticalities for both building vulnerability and damage, the population's and rescuers' routes conditions in evacuation strategies, and related safety levels. Such results can be represented through indices for the overall urban fabric as well as through risk-maps to quickly localize specific risks for each urban component (e.g. buildings, paths, assembly areas) by graphically representing them on the urban layout. The adopted KPIs are calculated according to EPES outputs. They can refer to each:

- *link* (Table 1) to represent its use by pedestrians and their interactions with other evacuees and debris. More links can be combined into an access route to evaluate their risk from the standpoint of the rescuers' actions;
- Codified Safe Area (CSA), in Table 2: evacuees' safety is connected to the minimization of directional variations and coming-and-going behaviours. Moreover, a CSA should contain evacuees in a safe environment, so overcrowding conditions and interactions with debris should be minimized within the CSA area. On the other hand,

rescuers might reach it after the earthquake: the analysis of access in aftermath conditions is linked to the possibility of moving towards the CSA by using an access route that is not blocked by debris and minimizes the interference with evacuees using the links and the presence of debris (Hashemi and Alesheikh 2013; Italian Technical Commission for Seismic Micro-zoning 2014; Hirokawa and Osaragi 2016; Zanini et al. 2017; Santarelli et al. 2018b). The ideal access route should be the shortest one that has the minimum interference conditions. In the case of access by emergency and rescue vehicles such as ambulances and fire trucks, a width route ≥3.5 m is suggested (Aguado et al. 2018); however, in historic urban fabric, this may not be possible for many alleys, so first responders can move only on foot;

[PLACE HERE TABLES 1 and 2]

- *Spontaneous Assembly Area* (SAA), in Table 3: since evacuees may decide to spontaneously gather outside a CSA for reasons of modifications to the surrounding environment or safety perception issues, rescuers in aftermath conditions may not be able to reach it, or may reach it only by using "dangerous" access routes. More than one access route should be defined when possible (at least two alternatives, taking into account what is reported above for CSA). Hence, the safety assessment should consider the possibility of the arriving evacuees remaining safe in it, depending on crowding and debris, and being rescued in the aftermath.

It is worth noting that some indices are normalized within the area data to define a priority list for interventions, by characterizing risk levels into 4 classes: low (0−0.25), medium-low (0.25−0.50), medium-high (0.50−0.75) and high (0.75−1).

2.4 ACT by proposing risk reduction solutions

The proposal of risk-mitigation strategies is based on the emergency evacuation process analysis and by taking advantage of the description of KPIs and the resulting risk maps (Bernardini et al. 2016; Maio et al. 2018; Robat Mili et al. 2018). According to different authors (Spence 2004; Hosseini et al. 2009; Egbelakin et al. 2011; Egbelakin et al. 2015; Ferreira et al. 2017b), related strategies can be based, for example, on: building retrofitting interventions; evacuation planning (i.e. location of assembly areas, rescuers' access routes, definition of evacuation paths); preparedness and population awareness; and emergency management, including support to the population (i.e. implementation of wayfinding signage, location of rescuers in the urban layout, etc.).

[PLACE HERE TABLE 3]

In this work, risk-mitigation strategies are considered to be implemented in the initial scenarios to create post-intervention scenarios and so to close the PDCA cycle by going back to the very first stage of the process (see Figure 1). The PDCA cycle can be repeated to evaluate the safety levels again, by means of KPIs and risk maps, to test the effectiveness of different risk-mitigation strategies. The main proposed KPIs to include for comparisons and the related general effectiveness criteria in post-intervention conditions are: $A_{eff,CSA}$ to be maximized; J_{SA} to be maximized by minimizing the number of CSA, by avoiding the formation of many SAA and by limiting the evacuation time, so as to focus rescuers' access (and by considering that $LOS_{CSA} \geq 0.3$ m^2/pp); V_{link}, T, $S_{link,CSA}$, S_{CSA} to be minimized; S_{SA} to be minimized by assisting people towards CSAs.

For each of these, the percentage difference *dx(%)* between different scenarios can be calculated according to Equation (9):

$$dx(\%) = \frac{x_{pi} - x_0}{x_0} \cdot 100 \quad (9)$$

where x is a general KPI, and the subscripts refer to the simulation in the original (subscript *0*) and post-intervention (subscript *pi*) conditions. Variation of the KPIs should be minimized or maximized to improve the safety levels depending on the considered KPI, as suggested by Tables 1, 2 and 3.

3 Case study and results

After a brief presentation of the case study in Section 3.1, two different simulation scenarios are presented and discussed in the present section. The first scenario, discussed in Section 3.2, corresponds to the current conditions of the study area. The second one, addressed in Section 3.3, considers the adoption of a series of risk reduction strategies specifically designed to mitigate the vulnerabilities identified in the first scenario. A critical comparison between the two scenarios is offered in Section 3.4 to evidence possible additional risk-mitigation strategies to be implemented according to a cyclic application of the framework shown in Figure 1.

3.1 The historic centre of Coimbra

The historic centre of Coimbra, in Portugal, is used in this work as a case study. The city of Coimbra is one of the oldest and most important Portuguese cities, especially for its historical and cultural significance (Vicente et al. 2015). The historic centre of Coimbra is characterised by a complex and irregular urban fabric with historic unreinforced masonry buildings that face narrow streets and winding alleys, thus being representative of many European historical city centres (see Figure 2). The majority of the buildings do not actually possess any seismic design or detailing and are therefore extremely vulnerable to a potential seismic event, even of a low to moderate intensity (Vicente et al. 2010).

[PLACE HERE FIGURE 2]

To provide the EPES input configuration, data from a 2D digital city map defined by the GIS tool are converted to a CAD file, by including the localization of the assumed codified assembly areas. The area included in the simulation is shown in Figure 3. This specific area is selected because of its critical conditions within the historic city centre. In particular, it presents an exceptionally irregular urban fabric, the seismic vulnerability of the buildings located in this area is especially high (see Figure 3), and the geometry of its boundaries offers particularly suitable conditions for the definition of *Codified Safe Areas* (CSA). In the simulation, it is also considered that no people from other parts of the city can move into this area. Such a premise can be considered as reasonable due to the position of the squares and other CSAs in the overall urban fabric (e.g. by considering evacuation strategies at the overall urban scale based on the definition of evacuation zones (Italian Technical Commission for Seismic Micro-zoning, 2014)).

3.2 Original scenario assessment

3.2.1 Original scenario characterization to PLAN and DO

Figure 3 (a) presents the buildings vulnerability map of the whole historic centre of Coimbra according to the previous work of Aguado et al. (2018), by distinguishing the main classes of the vulnerability index distribution. Figure 3 also highlights the buildings that are excluded from the vulnerability analysis (i.e. monuments or buildings for which the adopted vulnerability assessment method is not applicable).

[PLACE HERE FIGURE 3]

Figure 3 (b) focuses on the part of the urban fabric involved in the simulations carried out in this work, which, as noted before, is characterized by the generally high seismic vulnerability of the building façade walls associated with narrow streets and winding alleys. Such conditions imply many potential causes of interference with evacuation and rescue processes in an earthquake emergency (Gavarini 2001; Hirokawa and Osaragi 2016; Maio et al. 2018; Robat Mili et al. 2018).

Figure 4 (a) represents the urban path network, which is composed of 32 links divided by nodes codified by alphabetical letters, 8 possible final CSAs codified by related numbers, and 3 main access points to the area. In particular, since no data about a current emergency plan have been retrieved, the CSAs are considered to be located in wide urban fabric areas (i.e. squares, wide avenues), mainly preferring those at the boundaries of the areas, which, due to their peripheral location, can be directly reached by rescuers (i.e. those along the main roads).

[PLACE HERE FIGURE 4]

Moreover, Figure 4 (b) presents V_{link} values for each link. As can be seen in this figure, the most vulnerable links are links 7, 9, 10, 13, and inner parts of links 2 and 6 (characterized by the most vulnerable buildings, as shown by Figure 3). These links are the riskiest ones also for evacuation safety issues.

Finally, the investigated scenarios assume a possible seismic events severity of 5.6 Mw, which is the maximum historical local magnitude (Campos Costa et al. 2008) and a total number of inhabitants equal to 1200 (residents living in the area), distributed in the buildings according to Figure 5. Since only residents are simulated, it is assumed that all the evacuees know the position of the CSAs. The maximum evacuation time is fixed at 350 s, according to

Section 2.1.2. Since the evacuation paths are much shorter than 350 m and earthquake evacuation speeds are generally higher (see Section 2.1.2), this evacuation time can be considered as reasonable.

[PLACE HERE FIGURE 5]

3.2.2 CHECK original scenario by key performance indicators (KPIs)

3.2.2.1 Link and CSA assessment

Figure 6 (a) shows the evacuation curve of the whole considered area, with the average evacuation curve obtained in the simulations performed, together with the maximum and the minimum evacuation curves. As can be seen in Figure 6 (a), the maximum difference found between the maximum and minimum evacuation curves is equal to 5% (<10%). So, according to D'Orazio et al. (2014), it can be assumed that the analysis converges to an accurate solution. The average results show that 766 evacuees (64% of the hosted population) seem to be able to reach a CSA within the considered simulation time (350 s). Figure 6 (b) shows the evacuation curve for each CSA, while Table 4 summarizes the related CSA conditions in terms of the number of evacuees and their occupancy in safe conditions while waiting for rescuers to arrive.

[PLACE HERE FIGURE 6]

In general terms, the results confirm how the link vulnerability and the related effects on debris production (see Figure 7) can influence the evacuees' ability to reach a nearby CSA, since they are influenced in their path choice (blockage of paths to some CSAs) or slowed down (because of the reduced street width clear of debris and related evacuees–debris

repulsive forces in the SFM described in Appendix C), especially for the narrowest links (e.g. links 5 and 6 in Figure 4 (b)).

[PLACE HERE FIGURE 7]

The influence of the path blockage conditions is mainly retrieved for evacuees located in links 1, 22 and 23, who should move towards CSA2 and CSA6, for those along links 5 and 6 towards CSA4, and for those along links 14 and 15 towards CSA7. In particular, in all these conditions only the evacuees closest to the CSA can reach it in the shortest evacuation time (i.e. <50 s). In particular, the CSA2 data shows how this CSA is underused in comparison to its dimensions and the arriving individuals' occupancy conditions (compare to Table 4 LOS_{CSA} values for CSA2). In fact, since link 22 seems to be blocked (compare with Figure 7), individuals coming from links 1, 2, 8 and 24 prefer to aim for CSA5 and CSA6. The CSA2 occupancy suggests that evacuees who actually move towards CSA5 and CSA6 could be guided to reach CSA2, while reducing the blockage along link 22.

The majority of evacuees reach CSA0, as also shown by the highest J_{CSA} and LOS_{CSA} values in Table 4. CSA0 has a central position with respect to both the configuration of the urban fabric and a high density of inhabitants, while the surrounding links are generally characterized by significant damage conditions (see Figure 7) that could impede the evacuation towards other safe areas (i.e. CSA3 and CSA7). The slowing down of movement can be mainly seen for evacuees moving towards CSA1, CSA5 and CSA6, who come from the nearest links; although the overall paths are not much longer than the one to CSA2, the maximum evacuation time is higher. Similar effects are related to CSA3 and the related converging links 9, 10, 11 and 12, which are the longest ones in the area. Hence, the related J_{CSA} are higher than for the other CSAs, while the maximum evacuation time increases

because of debris-related slowing down effects. Despite the higher number of evacuees arriving, the related LOS_{CSA} conditions in Table 4 generally show a low occupancy level. The same conditions are seen for CSA8, by including the effects of the long link 10 without crossroads.

[PLACE HERE TABLE 4]

For each CSA, Table 5 summarises the sum of the final values of $S_{link,CSA}$, S_{CSA} and $S_{CSA,norm}$. In addition, Figure 8 shows the $S_{CSA,norm}$ values on the urban map and indicates the access routes for calculating $S_{link,CSA}$.

[PLACE HERE TABLE 5]

The values of $S_{link,CSA}$ for CSA2, CSA3, CSA4, CSA7 and CSA8 are equal to 0 since they are placed at the area boundaries and so are considered as being directly reached by rescuers coming from outside the studied area. According to the simulation results, CSA6 (and, secondly, CSA5) has the highest risk level because of the high number of pedestrians involved (moving on the street and waiting in the codified safe area) and the presence of debris, which additionally influences both the difference-in-path ratio and the safety link values.

[PLACE HERE FIGURE 8]

3.2.2.2 SAA assessment

The average number of evacuees who decide to gather in an SAA is about 316. The remainder cannot reach a CSA or gather in an SAA (10% of the overall number), and, at the end of the simulation time, they are located along the urban *links*.

Figure 9 shows the SAAs risk map by mainly indicating those areas with J_{SA}>5%: these SAAs contain 62% of all pedestrians gathering in SAAs. Figures 10 (a) and 10 (b) show the rescuers' two main access route alternatives: the choice is based on comparisons among the $S_{route,SAA}$ values. Table 6 summarises the related KPIs for them by finally providing S_{SAA} and $S_{SAA,norm}$ values. $S_{route,SAA}$ refers to the better alternative route among those shown in Figure 10 (b).

As suggested in previous works on real-world scenarios analysis (Bernardini et al. 2016), people gather in such SAAs because the path to a nearby CSA is blocked by debris or the surrounding conditions along the urban fabric are better in terms of damage levels and available space.

In narrow and very damaged areas, i.e. SAA0 and SAA6, evacuees seem to spontaneously gather at intermediate nodes. In particular, SAA0 is characterized by the worst conditions within the whole area because of the most significant presence of debris, which reduces the effective area where people can shelter in safe conditions (compare with $A_{eff,SAA}$ and $A_{debris,SAA}$ in Table 6). The same hazardous conditions characterize both the links converging to SAA0 and the possible access routes (see $S_{route,SAA}$ value).

Similar conditions are fundamental along the most vulnerable and longest links, i.e. for SAA1 and SAA2 (along link 2), SAA3 (along link 7), SAA7 and SAA8 (along link 10). According to Table 6, SAA2 is less safe than the next SAA1, mainly because of a significant risk in the SAAs (i.e., due to the presence of debris, see $S_{area,SAA}$ and smaller $A_{eff,SAA}$). On the contrary, SAA3 is more "dangerous" than the other nearby ones because the best choice of

access route to it is clearly influenced by debris and the evacuees' density conditions along it (i.e., people moving towards CSA3), as shown by the related $S_{route,SAA}$. As concerns SAA7 and SAA8, they may be affected by the vulnerability of minor facing buildings and, consequently, by a lesser presence of debris, as suggested by $A_{eff,SAA}$ and $S_{route,SAA}$. Nonetheless, since a similar value of $S_{route,SAA}$ has been obtained for the two alternative access routes, the shortest path is assumed to be the best one (rescuers' access from CSA8).

Finally, the simulations show that some of the evacuees can gather in areas which seem to be close to a CSA, as for SAA9 and SAA10, mainly because of slowing down phenomena in groups moving together (Tai et al. 2010; Bernardini et al. 2016).

[PLACE HERE TABLE 6]

[PLACE HERE FIGURES 9 AND 10]

3.2.3 ACT by proposing simulation-based risk mitigation strategy

According to the analysis of KPIs and to the general criteria of the risk-mitigation proposal defined in Section 2.1.4, the main strategies investigated in this work in order to increase safety levels are divided into two groups:

(i) *Buildings vulnerability interventions through retrofitting actions, starting from the most vulnerable ones located along the longer paths*. According to the simulation results, such a solution can potentially reduce evacuation and rescuers' issues related with debris generation by affecting the related T, $S_{path,CSA}$ and $S_{route,SAA}$ values. The 21 buildings highlighted in red in Figure 11 (a), located along critical links 4, 6, 7, 9 and

10, are selected. According to Ferreira et al. (2017b), the proposed techniques should mainly involve the improvement of:

a. wall-to-wall connections by means of effectively tying walls together with steel tie-rods;

b. wall-to-floor connections by means of the introduction of steel angle brackets adequately anchored to walls through steel connectors and anchor plates;

c. structural performance of the roofing system by introducing steel tie-rods underneath the ceiling joists;

(ii) *Evacuation management solutions*. The new plan of Figure 11 (b) is proposed to optimize the number and location of CSAs (smaller numbers and positions where evacuees can gather, so as to focus rescuers' action on fewer possible points of interest from the evacuees' standpoint). In particular:

a. CSA7 is removed because of its proximity to CSA0 and low J_{CSA}, supporting people to move towards CSA0 instead (i.e. plan dissemination actions, wayfinding signage);

b. CSA2 and CSA8 can be merged into a single CSA because both these CSAs are in the same large square within the urban fabric, and previous results indicate that neither of them seems to suffer from overcrowding;

c. a new CSA5 in Figure 11 (b) is considered instead of the original CSA6 and CSA5. It is located at the crossroad of two principal rescuers' paths (compare to Figure 8), and it could serve to accommodate evacuees from nearby links, as discussed in Section 3.1.2.1.

[PLACE HERE FIGURE 11]

3.3 Post-intervention scenario

3.3.1 Post-intervention scenario characterization to PLAN and DO

The post-intervention scenario is defined by implementing the solutions defined in Section 3.1.3. Table 7 compares the vulnerability index values, $I_{vf,}$ of the selected buildings identified in Figure 11 (a), in original and post-intervention conditions. Note that the building codes included in Table 7 refer to the identification provided in Figure 11 (a). The modifications of the buildings vulnerability indices influence the *urban path network vulnerability* of the related links 4, 6, 7, 9 and 10, which face the considered buildings. Table 7 provides the vulnerability values before and after the implementation of seismic retrofitting actions, while Table 8 compares the scenarios in terms of debris production on the related urban paths.

[PLACE HERE TABLES 7 AND 8]

These results show that the application of retrofitting strategies to a limited number of buildings can significantly reduce the vulnerability of the facing links (see Table 7). In debris production terms (see Table 8), the resulting effective area for pedestrians' movement increases within a typical historical scenario characterized by many narrow streets. The difference between the absolute values of both scenarios does not seem so substantial, thanks to the limited number of retrofitted buildings (Figure 7 remains representative of the scenario). Nevertheless, this can be crucial in ensuring safe paths for evacuees and safe access routes for rescuers.

The evacuation layout is defined according to Section 3.1.3 and shown in Figure 11. Finally, the earthquake magnitude, number and positions of inhabitants and maximum evacuation time are considered to be the same as in the original scenario.

3.3.2 CHECK post-intervention scenario by key performance indicators (KPIs)

This section summarises the post-intervention scenario simulation results, discussing them in relation to the implemented strategies. A complete comparison with the original scenario outcomes is provided in Section 3.3.

3.3.2.1 Link and CSA assessment

For the Section 3.1.2 results, Figure 12 (a) shows the evacuation curve for the whole considered area, by indicating the average, maximum, and minimum evacuation curves among the performed simulations and comparing them to the average evacuation curve for the original scenario conditions. As for the results in the original scenario, the difference between the maximum and minimum evacuation curves is acceptable, being equal to 4% (<10%). The average results show that 746 evacuees (62% of the accommodated population) seem to be able to reach a CSA within the considered simulation time (350 s), which is almost the same conditions as for the original scenario. Figure 12 (b) shows the evacuation curve to each CSA. Table 9 summarizes the related CSA occupancy conditions and Table 10 includes the ones used to calculate S_{CSA} and $S_{CSA,norm}$, by finally comparing the data with the original scenario conditions.

[PLACE HERE FIGURE 12]

The results confirm that a similar number of people to that of the original scenario conditions can gather in a reduced number of CSAs (see dJ_{CSA} data in Table 9), without a significant increase of LOS_{CSA} levels, or increasing the risk conditions along the access routes (see $\Sigma S_{link,CSA}$ data in Table 10).

[PLACE HERE TABLE 9]

The safety conditions of the CSA are quite similar, although some extreme conditions for evacuees' movement can be identified, due to debris production effects (see Figure 13), confirming the original scenario results. In particular, the risks for CSA4 are more evident in the original scenario. In fact, retrofitting actions on the two most vulnerable buildings along link 4 help to prevent blockage of the path, but J_{CSA} may increase by boosting negative interactions between evacuees and debris, as mainly shown by the T (and so S_{CSA}) higher values. For this reason, CSA4 now has $S_{CSA,Norm}$=100%.

[PLACE HERE FIGURE 13]

Figure 14 graphically summarises such $S_{CSA,norm}$ values over the study area and shows the access routes for calculating $S_{link,CSA}$.

[PLACE HERE TABLE 10]

[PLACE HERE FIGURE 14]

3.3.2.2 SAA assessment

The average number of evacuees who decide to gather in a SAA is about 320. This value is similar to that for the original scenario, but there are fewer SAAs, as shown in Figure 14 (b). Figure 14 (b) also shows the two main alternative access routes for rescuers. Table 11 summarises the related KPIs for them by finally providing the S_{SAA} and $S_{SAA,norm}$ values. $S_{route,SAA}$ refers to the best alternative route among those in Figure 8 (b). In Table 11, SAA0

and SAA1 can be respectively compared to SAA0 and SAA2 in the original scenarios because they are located in the same areas.

Firstly, the hazardous conditions at SAA0 are reduced in terms of the number of gathered individuals and the influence of debris, while $S_{route,SAA}$ increases because of the higher number of evacuees moving along the access route.

SAA1 in the post-intervention conditions has a higher risk than SAA2 in the original scenario, but this is mainly due to the significant increase in the number of individuals gathering and its effect on $S_{area,SAA}$. For this reason, SAA1 is the highest risk area in the post-intervention conditions. However, the absolute differences between the S_{SAA} values in the original and post-intervention conditions are quite slight and S_{SAA1} is half of S_{SAA0} in the original scenario.

Risk reduction interventions along link 10 make it possible to limit the formation of SAAs. Now people seem to spontaneously gather in SAA4 since they are slowed down by debris interference, but not blocked by it. The variation of the CSA position influences the evacuation process for the nearest area. The deletion of CSA7 leads to greater crowding in CSA0, while evacuees from areas near links 15, 16 and 20 prefer to gather in SAA6, which is located in a square. SAA6 can host them without significant interactions with debris (see related $A_{eff,SAA}$). However, S_{SAA6} is affected by the significant evacuees' usage conditions.

Finally, SAA1, SAA4 and SAA6 can be easily reached by rescuers, as indicated by the $S_{route,SAA}$ values in Table 11. Furthermore, they are also located very close to CSAs: gathering evacuees could be invited to continue their evacuation toward CSAs through, for instance, the adoption of wayfinding systems. Such results underline how the absolute S_{SAA} values are generally lower than those for the original conditions, demonstrating the effectiveness of the risk reduction strategies.

[PLACE HERE TABLE 11]

3.4 Critical comparison between the original and post-intervention scenarios and additional ACT proposals

This section compares the simulation results of the original and post-intervention scenarios through the use of KPIs and according to the implementation of the strategies referred to in Section 3.1.3, to show the main differences and improvements in the safety conditions, and to highlight possible additional solutions to be implemented according to the ACT rules in Section 2.1.4.

The reduction of CSAs, combined with retrofitting interventions on specific buildings, lead to evacuation improvements. On the one hand, the same number of evacuees arrive within a similar time at the CSA, according to the evacuation curves in Figure 12. Differences in the evacuation curves slope in Figure 12 are essentially due to the distances travelled by individuals to a CSA. From the rescuers' standpoint, evacuees gather in fewer CSAs, so actions can be better focused on them. Furthermore, access routes have a lower risk (see Table 9). On the other hand, evacuees−debris interactions are reduced. This result is most significant for the narrowest, most complex and longest links in the historical urban path network, as well as for the urban network areas hosting the most used SAAs. In this way, the movement and gathering conditions can be improved. The effects on links are mainly seen for: links 7, 8 and 9 towards CSA3 and CSA5 (reduction in difference-in-path ratio index and related reduction of S_{CSA}); and link 10 in relation to SAA4 (access route conditions). The effects on areas hosting SAAs are evidenced by an increase of the effective area (i.e., not occupied by debris), especially in SAA1 (see related $S_{area,SAA}$ in Table 11).

Finally, the analysis of the post-intervention conditions makes it possible to determine how some additional strategies should be implemented. Figure 15 offers an additional plan for the historic part of Coimbra based on the following notes:

- Despite the optimization of their positions and number, the CSAs are not fully exploited in terms of their capacity to accommodate people. An additional selection of CSAs could be undertaken (e.g. merging CSA1 and CSA5 to also try to gather evacuees from SAA6). However, many SAAs are now very close to a CSA (i.e. SAA1 and CSA5; SAA4 and CSA3): this suggests that wayfinding strategies could be implemented to get people to move towards the nearest CSA (Bernardini et al. 2016). In particular, evacuation signs could be installed along the paths or a small group of first responders could be sent immediately to such an SAA (i.e. see green arrows in Figure 15).

[PLACE HERE FIGURE 15]

- As shown in Figure 15, further retrofitting interventions could involve additional buildings along critical links, i.e. links 9 and 10, since they connect CSA3, and link 7, since this remains the most vulnerable one in the area (compare to Table 8). Economic analyses for supporting public−private partnerships in such operations could be evaluated to define the sustainability optimization of such solutions. Analyses on the selected area of the historic centre of Coimbra should be combined with others in surrounding parts of the overall historical urban fabric. The division within sectors (for simulation and emergency management purposes) could be more effective to plan focused and agile solutions also by involving different input scenario configurations (i.e. earthquake magnitude, hosted population). Boundaries between sectors (and related CSAs on the boundary), should nevertheless be jointly analysed as far as possible.

4 Limitations and future directions

This work is a first attempt to demonstrate the capabilities of the proposed holistic simulation-based methodology through a significant case study application. Hence, in this first research step, a simplified approach to the definition of some behavioural inputs in an evacuation simulation has been adopted, by trying to replicate the input conditions from previous evacuation simulation tool validation processes. On the one hand, this choice ensures the consistency of results with those of previous works. On the other hand, the application of the simulation tools is mainly affected by certain behaviour-related limitations, and, in particular by: (a) the evacuation speed; (b) the representation of behavioural choices (i.e. choice of evacuation path). As concerns the evacuation speed, the work uses data from real-world earthquake scenarios, limiting the adoption of values from general purpose or non-specific disasters (e.g. fires or floods) databases. In this way, the effects of earthquakes on the human response can be identified. Nevertheless, the simulations performed do not consider the effects on individuals' speed due to age and mobility issues, or of surrounding environment conditions (e.g. lighting levels). This choice is essentially due to the current lack of data on such issues in earthquake evacuation conditions. Different simulation setups will have to be performed to verify the impact of such features on the final evacuation results and on the effectiveness of the risk-reduction solutions. As concerns evacuation choices and the adopted related stochastic error, the current value of 10% is consistent with the probabilities of using or changing the evacuation direction used in microscopic simulations and adopted in the simulator validation. However, it could be possible to perform simulations with different stochastic errors, so as to highlight the final impact of different behavioural choices on the final evacuation result, so as to manage different uncertainty levels of inputs and correlate them with stochastic outputs (e.g. Monte Carlo simulations).

Another evacuation simulation limitation relates to path blockage estimation. In this work, a deterministic approach for debris estimation has been used according to the methods of Santarelli et al. (2018), which are dependent on the earthquake severity. Such deterministic approaches are simple and quick to use, and they are also commonly adopted by other earthquake risk assessment approaches (e.g. (Italian Technical Commission for Seismic Micro-zoning 2014; Zanini et al. 2017)). Future works should support a probabilistic approach to damage assessment and path blockage, by additionally investigating the interactions between the evacuees and the debris (e.g. reducing the evacuation speed when walking through different surrounding debris conditions (Lu et al. 2019)). From this point of view, the effects of shaking intensity or distance can be included by also adopting approaches that use ground velocity/acceleration to estimate the damage in post-earthquake conditions.

Finally, the current application is limited to an area of the historical city centre, mainly because of the limits in simulations of the adopted software. Although the application to a limited city area seems not to affect the demonstration of the capability of the proposed method and of the microscopic simulation modelling approach used, future research should overcome this limitation by considering entire city sections (e.g. the whole historical city centre). Moreover, in order to derive some general rules and trends in the evacuation process, it is important to apply this methodology to other case studies. The investigation of the impact of different retrofitting solutions should involve the improvement and/or the consideration of some additional aspects, such as: (a) a deeper sociodemographic characterization; (b) different individuals' awareness levels towards the emergency procedure and plan; (c) and the interaction of evacuees with wayfinding and rescuers' movements (including vehicle access) or operations.

5 Final remarks

An original simulation-based methodology focused on urban evacuation paths and assembly areas for different earthquake scenarios is proposed in this paper. Recognising the role of the external environment on the evacuation process, a validated urban earthquake pedestrians' evacuation simulation software is used to retrieve and compare probable behaviours and movement decisions in relation to different environmental conditions, including damage conditions and different emergency management decisions. In this way, the proposed procedure for the first time combines vulnerability and human behaviour to evaluate the evacuation safety conditions of a historic urban area, and then to accordingly assess the related criticalities.

Criteria and key performance indicators (KPIs) for safety assessment are defined to organize the simulation results and a series of risk maps are then created to represent the safety conditions of the urban layout analysed. Finally, different risk-reduction strategies, including management and retrofitting actions, are provided and analysed from a holistic perspective.

The results obtained in this work prove the capabilities of the methodology proposed in this paper. In particular, the proposed KPIs can provide a quantitative support to safety and buildings designers, urban planners, civil protection organizations and decision-makers, while assessing the impact of different risk-mitigation strategies. The proposed methodology also underlines how such strategies can be checked by a cycle-based approach. In each scenario condition, it is possible to point out, for example, which areas can be effectively used by individuals and so how to modify/integrate the assembly points plan; which strategies could improve the number of people arriving in safe areas and/or diminish the risk levels for evacuees; which rescuers' actions should be carried out to support and reach people in the evacuation process, by assigning a priority level to each of them. Furthermore, such

risk analysis methodologies could be combined with additional assessment variables (e.g. cost assessment for the proposed strategies at both urban and single-building scales; social vulnerability aspects) so as to move towards a more comprehensive community resilience assessment in the given scenario.

As a final note, it is worth noting that this approach can be easily adapted and applied to assess other type of hazards at the urban scale (e.g. flood, fires, heatwaves, etc.), as well as in non-historic contexts.

Appendix A: Notation table

[PLACE HERE TABLE A1]

Appendix B: Seismic building vulnerability assessment

The vulnerability assessment method used in this work was proposed by Ferreira et al. (2014). The method concerns historic masonry buildings and uses data from external analyses of façade walls. The seismic vulnerability of the façade wall can be calculated as the weighted sum of 13 evaluation parameters listed in Table B1, and then normalized to range between 0 and 100. The parameters described in Table B1 have been calibrated on Portuguese case studies (Ferreira et al. 2017a).

[PLACE HERE TABLE B1]

Appendix C: Evacuation path network conditions assessment

Based on the vulnerability of the façade walls defined in Appendix B, the Street Vulnerability Index proposed by Santarelli et al. (2018b) is used to assess safety conditions for pedestrians' evacuation along the paths based only on buildings vulnerability. This index considers the vulnerability of buildings facing each street, by also including their effective incidence on the

path length. The street urban network is composed of nodes that are placed at crossroads and squares or, generally, in each significant plan variation along the streets. Hence, links represent parts of the street network between pairs of nodes. The vulnerability index is calculated for each link according to Equation (C.1):

$$V_{link} = \sum(I_{vf} \times i) \quad \text{(C.1)}$$

where $\boldsymbol{I_{vf}}$ [-] is the normalized vulnerability index of the façade wall (Ferreira et al. 2017a) and i represents the ratio between the length of the façade wall and the total length of the link. This method generates an absolute index because of the adopted vulnerability estimation methodology; thus, different vulnerability indices from different urban scenarios (e.g. original conditions and post-intervention conditions) can be compared within the same vulnerability ranking.

This index evaluation makes it possible to identify the most vulnerable links in the urban streets network, but it does not supply any information about the possibility that a given path could be blocked by debris during the evacuation phases, and neither is it a function of the earthquake intensity. Therefore, the probability of path blockages is offered by calculation of the depth of debris along the street in terms of the effective occupied area, as performed by the simulator and presented in Section 2.1.3.

Appendix D: Earthquake Pedestrians' Evacuation Simulator

The Earthquake Pedestrians' Evacuation Simulator (EPES), developed and validated in previous works for historical city centres evacuation simulation (D'Orazio et al. 2014), is used to perform evacuation simulations. EPES uses a combined ABM-SFM model to solve pedestrians–pedestrians and pedestrians–built environment interactions in emergency conditions.

In the ABM model, the built "environment" is modelled as a specific agent, and so criteria for earthquake-induced modifications can be autonomously described. The original rules are based on a rough and discrete quantification of building debris according to the building vulnerability and earthquake EMS-98 intensity. In the adopted EPES version, the building debris on urban paths d_{debris} [m] proposed by Santarelli et al. (2018a) is introduced to include continuous and experimentally validated debris estimation criteria. This magnitude-based method has been adopted in this preliminary work because of its limited computational cost during both the PLAN phases activities (collecting data on the building vulnerability to be used in assessing the building damage) and the DO phase (reduced computational simulation costs for wide areas in the current EPES version). However, the debris depth assessment criteria could be replaced by any other approach, as for the other simulation methods in Section 2. For each building, the input values of the method are:

- buildings vulnerability V_F [-], determined according to (Ferreira et al. 2014);
- magnitude ratio R_M [-], that varies from 0 to 1 and is the ratio between the seismic event moment magnitude and the maximum expected magnitude (equal to 9.5 according to the world seismic history);
- the ratio between the building height and facing street geometry *h/W* [-].

The inputs are combined as shown by Equation (D.1) to define the modified vulnerability index V_F^* [-], which includes the three factors.

$$V_F^* = V_F \cdot R_M \cdot {}^{h}\!/_{W} \quad \text{(D.1)}$$

Finally, for each building, Equation (D.2) calculates d_{debris} [m] as a function of V_F^* and the width W of the facing street [m]. The debris distribution is constant for all of the building side along the considered street.

$$d_{debris}^{pred} = \begin{cases} \left(213.09 \cdot V_F^*/100\right) \cdot W\,, & , V_F^* \leq 0.47 \\ W, & V_F^* > 0.47 \end{cases} \quad \text{(D.2)}$$

The method and Equation (D.2) are validated according to real-world data by considering different exceedance probabilities. As stated by Santarelli et al. (2018a), the exceedance probability can represent the desired level of safety for planning and the respective percentage errors of the accuracy of the debris assessment. Equation (D.2) can estimate the effective debris depth with an accuracy on average real-world debris depth values equal to +80% (overestimation of debris depth), when considering an exceedance probability of 75%, and -13% (slight underestimation of debris depth), when considering an exceedance probability of 50%. Hence, these conditions represent an average damage scenario for the assumed earthquake magnitude. The slight underestimation difference can be assumed to reflect the possibility that people can walk over the extreme debris areas (those further from the damaged building) (Bernardini et al. 2016; Lu et al. 2019). As concerns the pedestrians' evacuation criteria, the motion of each simulated individual is influenced by the decisions of surrounding evacuees, debris, and historical building and path features. According to the SFM approach (Helbing and Johansson 2010), each pedestrian moves in a "forces field" characterized by repulsive forces from obstacles $\overrightarrow{F_{rep,w}}$ [N] (i.e. obstacles and debris avoidance; keeping a safe distance from buildings and debris) and people $\overrightarrow{F_{rep,i}}$ [N] (i.e. avoiding physical contact) and attractive forces from the evacuation target $\overrightarrow{O_g(t)}$ (i.e. the desire to reach an assembly area) and from other individuals $\sum\overrightarrow{F_{attr,i}(t)}$ (i.e. social attachment between evacuees in the same group) and phenomena. Synthetically, the individual tries to match his/her preferred speed to such forces. Equation (D.3) summarises the SFM motion equation, where the individual's acceleration $\frac{\overrightarrow{dv_i(t+dt)}}{dt}$ [m/s^2] at the instant of time *t* depends on the aforementioned resulting forces and on their random variation $\overrightarrow{\varepsilon(t)}$ [N]. Equation (D.3) is solved for each simulated pedestrian at each simulation time.

$$m_i\frac{\overrightarrow{dv_i(t+dt)}}{dt} = \overrightarrow{O_g(t)} + \sum\overrightarrow{F_{rep,i}(t)} + \sum\overrightarrow{F_{rep,w}(t)} + \sum\overrightarrow{F_{attr,i}(t)} + \overrightarrow{\varepsilon(t)} \quad \text{(D.3)}$$

Equation (D.4) summarises the evacuation target attractive force, which depends on the individual's: mass m_i [kg]; preferred speed $v_{pref,i}(t)$ [m/s]; velocity at the next simulation step $\overrightarrow{v_i(t+dt)}$ [m/s]; reaction time τ_i [s]; dt [s] is the time difference between two consecutive calculation instants.

$$\overrightarrow{O_g} = \frac{m_i\left(v_{pref,i}(t)\overrightarrow{e_i(t)} - \overrightarrow{v_i(t+dt)}\right)}{\tau_i} \quad \text{(D.4)}$$

As concerns decisional rules included in the ABM, the choice of evacuation path in "spontaneous" evacuation conditions (considering no wayfinding elements, so without any specified paths to be used) is influenced by the following non-dimensional parameters:

- paths geometry in terms of: $R_{W/h}$ - average *W/h* ratio along the path; d_s - ratio between geometric distances of pedestrian's shortest evacuation path and the considered path *p*;
- visible damage levels of the path in terms of: $A_{l,p}$ - ratio between the path area without debris and the total path area; L_p - ratio between *p* average width and the largest selectable path, by considering debris depth on them;
- social effects in terms of N_p - ratio between the number of people moving along *p* and the total number of visible surrounding pedestrians;
- the support of wayfinding elements (i.e. presence of rescuers or wayfinding signage or level of knowledge of the evacuation plan) by the term O_p (binary value: 0 - no wayfinding support or 100 - support presence). When no support of wayfinding elements is present in any path (i.e. in "spontaneous" conditions), $O_p=100$ for all the paths.
- level of knowledge of urban spaces, by considering M_p - memory effects on the considered path.

The evacuation direction choice is made when the simulated individual is placed in an intersection between paths, i.e. crossroads and path plano-altimetric variations. A choice probability P_p [%] is calculated according to such parameters and expressed in percentage terms according to Equation (D.5) (variable from 0% - the path will be not chosen, to 100% - all the people will follow the path).

$$P_p = R_{W/h} \cdot d_s \cdot L_p \cdot A_{l,p} \cdot N_p \cdot O_p \cdot M_p \,[\%] \quad \text{(D.5)}$$

The pedestrians choose the path with the higher P_p values. However, if more than one available path has the same P_p, the simulated pedestrian will randomly choose one of them. If the path from which the evacuees come has a P_p greater than the possible alternatives, the individual can go back (a maximum of 3 times). A stochastic error (10%) is introduced to describe behavioural differences between individuals about this path selection criterion. In simulations: $\tau_i = 0.5\ s$, dt=0.1 s, m_i=80 kg, M_p=*100* (considering people familiar with the urban layout) and attractive/repulsive forces are activated for elements within 3 m from the evaluated individual. Finally, EPES has been implemented at *Università Politecnica delle Marche* as a Java simulation tool, which currently operates by using a single-thread execution which limits the area and number of agents that can be simulated.

Acknowledgments

The work presented in this article was supported by the European Union within the framework of the Erasmus Mundus Advanced Master in Structural Analysis of Monuments and Historical Constructions (SAHC) and by the Portuguese Foundation for Science and Technology (FCT) through the postdoctoral fellowship SFRH/BPD/ 122598/2016. The authors would like to express their sincere gratitude to the editor and the two anonymous reviewers for their insightful and constructive comments.

References

Aguado JLP, Ferreira TM, Lourenço PB (2018) The Use of a Large-Scale Seismic Vulnerability Assessment Approach for Masonry Façade Walls as an Effective Tool for Evaluating, Managing and Mitigating Seismic Risk in Historical Centers. International Journal of Architectural Heritage 12:1259–1275. doi: 10.1080/15583058.2018.1503366

Anastasiadis A, Argyroudis S (2007) Seismic vulnerability analysis in urban systems and road networks. Application to the city of Thessaloniki, Greece. International Journal of Sustainable Development and Planning 2:287–301. doi: 10.2495/SDP-V2-N3-287-301

Barbat AH, Carreno ML, Pujades LG, et al (2010) Seismic vulnerability and risk evaluation methods for urban areas. A review with application to a pilot area. Structure and Infrastructure Engineering 6:17–38. doi: 10.1080/15732470802663763

Bernardini G, D'Orazio M, Quagliarini E (2016) Towards a "behavioural design" approach for seismic risk reduction strategies of buildings and their environment. Safety Science 86:273–294. doi: 10.1016/j.ssci.2016.03.010

Campos Costa A, Sousa ML, Carvalho A (2008) Seismic Zonation for Portuguese National Annex of Eurocode 8. Proceedings of the 14th World Conference on Earthquake Engineering, Beijing, China 8–15.

Cer G, Rezgui Y, Zhao W (2017) Critical review of existing built environment resilience frameworks: Directions for future research. International Journal of Disaster Risk Reduction 25:173–189. doi: 10.1016/j.ijdrr.2017.09.018

Chu H, Yu J, Wen J, et al (2019) Emergency Evacuation Simulation and Management Optimization in Urban Residential Communities. Sustainability 11(3): 795. doi: 10.3390/su11030795

Comerio MC (2004) Public policy for reducing earthquake risks: a US perspective. Building Research & Information 32:403–413. doi: 10.1080/0961321042000221052

D'Amico A, Currà E (2014) The Role of Urban Built Heritage in Qualify and Quantify Resilience. Specific Issues in Mediterranean City. Procedia Economics and Finance 18:181–189. doi: 10.1016/S2212-5671(14)00929-0

D'Orazio M, Quagliarini E, Bernardini G, et al (2014) EPES - Earthquake pedestrians' evacuation simulator: A tool for predicting earthquake pedestrians' evacuation in urban outdoor scenarios. International Journal of Disaster Risk Reduction 10:153–177. doi: 10.1016/j.ijdrr.2014.08.002

Dilley M, Chen RS, Deichmann U, et al (2005) Natural Disaster Hotspots. A Global Risk Analysis. Washington, DC: World Bank. http://documents.worldbank.org/curated/en/621711468175150317/Natural-disaster-hotspots-A-global-risk-analysis

Dolce M, Speranza E, Bocchi F, et al (2018) Probabilistic assessment of structural operational efficiency in emergency limit conditions: the I.OPà.CLE method. Bulletin of Earthquake Engineering 16:3791–3818. doi: 10.1007/s10518-018-0327-7

Dong B, Yan D, Li Z, et al (2018) Modeling occupancy and behavior for better building design and operation - A critical review. Building Simulation 11:899–921. doi: 10.1007/s12273-018-0452-x

Egbelakin T, Wilkinson S, Potangaroa R, et al (2015) Stakeholders' practices: a challenge to earthquake risk mitigation decisions. International Journal of Strategic Property Management 19:395–408. doi: 10.3846/1648715X.2015.1101029

Egbelakin TK, Wilkinson S, Potangaroa R, et al (2011) Challenges to successful seismic retrofit implementation: a socio-behavioural perspective. Building Research & Information 39:286–300. doi: 10.1080/09613218.2011.552264

Ferreira TM, Costa AA, Costa A (2015) Analysis of the Out-Of-Plane Seismic Behavior of Unreinforced Masonry: A Literature Review. International Journal of Architectural

Heritage. 9(8): 949-972. doi: 10.1080/15583058.2014.885996

Ferreira TM, Maio R, Costa AA, et al (2017a) Seismic vulnerability assessment of stone masonry façade walls: Calibration using fragility-based results and observed damage. Soil Dynamics and Earthquake Engineering 103: 21-37. doi: 10.1016/j.soildyn.2017.09.006

Ferreira TM, Maio R, Vicente R (2017b) Analysis of the impact of large scale seismic retrofitting strategies through the application of a vulnerability-based approach on traditional masonry buildings. Earthquake Engineering and Engineering Vibration 16:329–348. doi: 10.1007/s11803-017-0385-x

Ferreira TM, Vicente R, Raimundo Mendes da Silva JA, et al (2016) Urban fire risk: Evaluation and emergency planning. Journal of Cultural Heritage 20:739–745. doi: 10.1016/j.culher.2016.01.011

Ferreira TM, Vicentea R, Varum H (2014) Seismic vulnerability assessment of masonry facade walls: development, application and validation of a new scoring method. Structural Engineering and Mechanics 50:541–561. doi: 10.12989/sem.2014.50.4.541

Filippova O, Xiao Y, Rehm M, et al (2018) Economic effects of regulating the seismic strengthening of older buildings. Building Research & Information 46:711–724. doi: 10.1080/09613218.2017.1357318

Francini M, Artese S, Gaudio S, et al (2018) To support urban emergency planning: A GIS instrument for the choice of optimal routes based on seismic hazards. International Journal of Disaster Risk Reduction 31:121–134. doi: 10.1016/j.ijdrr.2018.04.020

French EL, Birchall SJ, Landman K, et al (2018) Designing public open space to support seismic resilience: A systematic review. International Journal of Disaster Risk Reduction 32: 1-10. doi: 10.1016/J.IJDRR.2018.11.001

Gavarini C (2001) Seismic risk in historical centers. Soil Dynamics and Earthquake

Engineering 21:459–466. doi: 10.1016/S0267-7261(01)00027-6

Grünthal G (1998) European Macroseismic Scale 1998. European Center of Geodynamics and Sismology, Bruxels.

Hashemi M, Alesheikh AA (2013) GIS: agent-based modeling and evaluation of an earthquake-stricken area with a case study in Tehran, Iran. Natural Hazards 69:1–23. doi: 10.1007/s11069-013-0784-x

Helbing D, Johansson AF (2010) Pedestrian, Crowd and Evacuation Dynamics. Encyclopedia of Complexity and Systems Science 16:6476–6495. doi: 10.1007/978-0-387-30440-3_382

Hirokawa N, Osaragi T (2016) Earthquake disaster simulation system : Integration of models for building collapse, road blockage, and fire spread. Journal of Disaster Research 11:175–187. doi: 10.20965/jdr.2016.p0175

Hosseini KA, Jafari MK, Hosseini M, et al (2009) Development of urban planning guidelines for improving emergency response capacities in seismic areas of Iran. Disasters 33:645–664. doi: 10.1111/j.1467-7717.2008.01092.x

Hubbard S, Stewart K, Fan J (2014) Modeling spatiotemporal patterns of building vulnerability and content evacuations before a riverine flood disaster. Applied Geography 52:172–181. doi: 10.1016/j.apgeog.2014.05.006

Ismail-Zadeh A, Soloviev A, Sokolov V, et al (2017) Quantitative modeling of the lithosphere dynamics, earthquakes and seismic hazard. Tectonophysics 746: 624-647. doi: 10.1016/j.tecto.2017.04.007

Italian technical commission for seismic micro-zoning (2014) Handbook of analysis of emergency conditions in urban scenarios (Manuale per l'analisi della condizione limite dell'emergenza dell'insediamento urbano (CLE); in Italian), 1st edn. Rome, Italy

Kimms A, Maiwald M (2018) Bi-objective safe and resilient urban evacuation planning.

European Journal of Operational Research 269:1122–1136. doi: 10.1016/j.ejor.2018.02.050

Korhonen T, Hostikka S (2010) Fire Dynamics Simulator with Evacuation: FDS + Evac Technical Reference and User's Guide.

Kuligowski ED (2016) Computer Evacuation Models for Buildings. In: SFPE Handbook of Fire Protection Engineering. Springer New York, New York, NY, pp 2152–2180

Lagomarsino S, Giovinazzi S (2006) Macroseismic and mechanical models for the vulnerability and damage assessment of current buildings. Bulletin of Earthquake Engineering 4:415–443. doi: 10.1007/s10518-006-9024-z

Lämmel G, Grether D, Nagel K (2010) The representation and implementation of time-dependent inundation in large-scale microscopic evacuation simulations. Transportation Research Part C: Emerging Technologies 18:84–98. doi: 10.1016/j.trc.2009.04.020

Lombardo G, Cicero C (2015) Analysis of seismic vulnerability for urban centres. International Journal of Design Sciences and Technology 1:39–58.

Lu X, Yang Z, Cimellaro GP, et al (2019) Pedestrian evacuation simulation under the scenario with earthquake-induced falling debris. Safety Science 114:61–71. https://doi.org/10.1016/J.SSCI.2018.12.028

Macal CM, North MJ (2010) Tutorial on agent-based modelling and simulation. Journal of Simulation 4:151–162. doi: 10.1057/jos.2010.3

Maio R, Ferreira TM, Vicente R (2018) A critical discussion on the earthquake risk mitigation of urban cultural heritage assets. International Journal of Disaster Risk Reduction 27:239–247. doi: 10.1016/j.ijdrr.2017.10.010

Moore T (2008) BIP 2034:2008 - Disaster and Emergency Management Systems. British Standards Institution, London, UK

O'Brien W, Gaetani I, Carlucci S, et al (2017) On occupant-centric building performance

metrics. Building and Environment 122:373–385. doi: 10.1016/j.buildenv.2017.06.028

Okaya M, Takahashi T (2015) Evacuation Guidance and Agent Behavior in Evacuation Simulations. Electronics and Communications in Japan 98(10): 41–48. https://doi.org/10.1002/ecj.11731

Oki T, Osaragi T (2017) Urban Improvement Policies for Reducing Human Damage in a Large Earthquake by Using Wide-Area Evacuation Simulation Incorporating Rescue and Firefighting by Local Residents. In: Geertman S, Allan A, Pettit C, Stillwell J (eds) Planning Support Science for Smarter Urban Futures. Springer International Publishing, Cham, pp 449–468

Ortiz R, Ortiz P (2016) Vulnerability Index: A New Approach for Preventive Conservation of Monuments. International Journal of Architectural Heritage 10:1078–1100. doi: 10.1080/15583058.2016.1186758

Pace B, Boncio P, Brozzetti F, et al (2008) From regional seismic hazard to "scenario earthquakes" for seismic microzoning: A new methodological tool for the Celano Project. Soil Dynamics and Earthquake Engineering 28:866–874. doi: 10.1016/j.soildyn.2007.11.001

Parisi DR, Dorso CO (2005) Microscopic dynamics of pedestrian evacuation. Physica A: Statistical Mechanics and its Applications 354:606–618. doi: 10.1016/j.physa.2005.02.040

Quagliarini E, Bernardini G, Santarelli S, et al (2018) Evacuation paths in historic city centres: A holistic methodology for assessing their seismic risk. International Journal of Disaster Risk Reduction 31:698–710. doi: 10.1016/j.ijdrr.2018.07.010

Robat Mili R, Amini Hosseini K, Izadkhah YO (2018) Developing a holistic model for earthquake risk assessment and disaster management interventions in urban fabrics. International Journal of Disaster Risk Reduction 27:355–365. doi:

10.1016/j.ijdrr.2017.10.022

Ronchi E, Kuligowski ED, Reneke PA, et al (2013) The Process of Verification and Validation of Building Fire Evacuation Models. Technical Note (NIST TN) - 1822. doi: 10.6028/NIST.TN.1822

Santarelli S, Bernardini G, Quagliarini E (2018a) Earthquake building debris estimation in historic city centres: From real world data to experimental-based criteria. International Journal of Disaster Risk Reduction 31:281–291. doi: 10.1016/j.ijdrr.2018.05.017

Santarelli S, Bernardini G, Quagliarini E, D'Orazio M (2018b) New Indices for the Existing City-Centers Streets Network Reliability and Availability Assessment in Earthquake Emergency. International Journal of Architectural Heritage 12:153–168. doi: 10.1080/15583058.2017.1328543

Schadschneider A, Klingsch W, Klüpfel H, et al (2009) Evacuation Dynamics: Empirical Results, Modeling and Applications. Encyclopedia of Complexity and Systems Science 3142–3176 LA–English.

Shrestha SR, Sliuzas R, Kuffer M (2018) Open spaces and risk perception in post-earthquake Kathmandu city. Applied Geography 93:81–91. doi: 10.1016/J.APGEOG.2018.02.016

Song, Y., Xie, K., & Su, W. (2019). Mechanism and strategies of post-earthquake evacuation based on cellular automata model. International Journal of Disaster Risk Reduction 34:220–231. https://doi.org/10.1016/j.ijdrr.2018.11.020

Spence R (2004) Risk and regulation: can improved government action reduce the impacts of natural disasters? Building Research & Information 32:391–402. doi: 10.1080/0961321042000221043

Tai C-A, Lee Y-L, Lin C-Y (2010) Urban Disaster Prevention Shelter Location and Evacuation Behavior Analysis. Journal of Asian Architecture and Building Engineering 9:215–220. doi: 10.3130/jaabe.9.215

Thompson P-A, Marchant EW (1995) Testing and application of the computer model 'SIMULEX.' Fire Safety Journal 24(2):149–166. doi: 10.1016/0379-7112(95)00020-T

Thompson P, Nilsson D, Boyce K, et al (2015) Evacuation models are running out of time. Fire Safety Journal 78:251–261. doi: 10.1016/j.firesaf.2015.09.004

Vicente R, Ferreira T, Maio R (2014) Seismic Risk at the Urban Scale: Assessment, Mapping and Planning. Procedia Economics and Finance 18:71–80. doi: 10.1016/S2212-5671(14)00915-0

Vicente R, Ferreira TM, Mendes da Silva JAR (2015) Supporting urban regeneration and building refurbishment. Strategies for building appraisal and inspection of old building stock in city centres. Journal of Cultural Heritage 16(1): 1-14. doi: 10.1016/j.culher.2014.03.004

Vicente R, Parodi S, Lagomarsino S, et al (2010) Seismic vulnerability and risk assessment: case study of the historic city centre of Coimbra, Portugal. Bulletin of Earthquake Engineering 9:1067–1096. doi: 10.1007/s10518-010-9233-3

Villagra P, Rojas C, Ohno R, et al (2014) A GIS-base exploration of the relationships between open space systems and urban form for the adaptive capacity of cities after an earthquake: The cases of two Chilean cities. Applied Geography 48:64–78. doi: 10.1016/j.apgeog.2014.01.010

Xiao M-L, Chen Y, Yan M-J, et al (2016) Simulation of household evacuation in the 2014 Ludian earthquake. Bulletin of Earthquake Engineering 14:1757–1769. doi: 10.1007/s10518-016-9887-6

Yu J, Zhang C, Wen J, et al (2018), Integrating Multi-agent Evacuation Simulation and Multi-criteria Evaluation for Spatial Allocation of Urban Emergency Shelters, International Journal of Geographical Information Science 32(9): 1884-1910.

Zanini MA, Faleschini F, Zampieri P, et al (2017) Post-quake urban road network

functionality assessment for seismic emergency management in historical centres. Structure and Infrastructure Engineering 13:1117–1129. doi: 10.1080/15732479.2016.1244211

Figure Captions

Figure 1. Proposed operational framework according to the PDCA cycle (Moore 2008; Bernardini et al. 2016).

Figure 2. Overview of the Historic Centre of Coimbra (left: photo of the authors) and view to an inner street (right: photo of the authors).

Figure 3. Vulnerability maps: (a) global vulnerability distribution over the Historic Centre of Coimbra; (b) study area and identification of the building facade walls with vulnerability index values higher than 45.

Figure 4. Study area: (a) network schematization; (b) V_{links} representation, by including which safe areas are directly accessed in emergency conditions (symbol: =>).

Figure 5. Hosted inhabitants within the area buildings.

Figure 6. Original scenario evacuation curve results: (a) average, minimum and maximum curves for the whole area; (b) Evacuation curves obtained for each CSA.

Figure 7. Building debris generation in the original scenario (Percentage from the total link area, occupied by debris).

Figure 8. CSA risk map: risk levels for CSA, rescuers' access points to the area (=>) and related rescuers' access routes to CSA (blue lines over links) on the urban layout map.

Figure 9. SA risk maps in original scenario conditions (SAs where J_{SA}>5% are marked by a coloured circle) risk characterization (circle radius roughly define a priority in the $S_{SA,norm}$ values).

Figure 10 Routes to reach CSA (a) worse routes to reach each CSA; (b) better routes to reach each CSA.

Figure 11 Proposal of risk-mitigation strategies: (a) building selected for retrofit intervention by including related identification codes; (b) proposed evacuation plan with CSA location.

Figure 12 Post-intervention scenario evacuation curve results:-a Average, minimum and maximum curves for the whole area compared to the original scenario average curve;-b Evacuation curves obtained for each considered CSA according to Figure 11 definition.

Figure 13 Building debris generation in the post-intervention scenario.

Figure 14 Analysis of the improved urban scenario: (a) risk levels for CSA, rescuers' access points to the area (see =>) and related rescuers' access routes to CSA (blue lines over links) on the urban layout map; (b) SAs risk characterization and identification of the best paths to reach SA.

Figure 15 Proposal of additional risk-mitigation strategies on the post-intervention scenario, by defining possible wayfinding solutions, additional retrofit interventions and proposed access routes to CSA and SA.

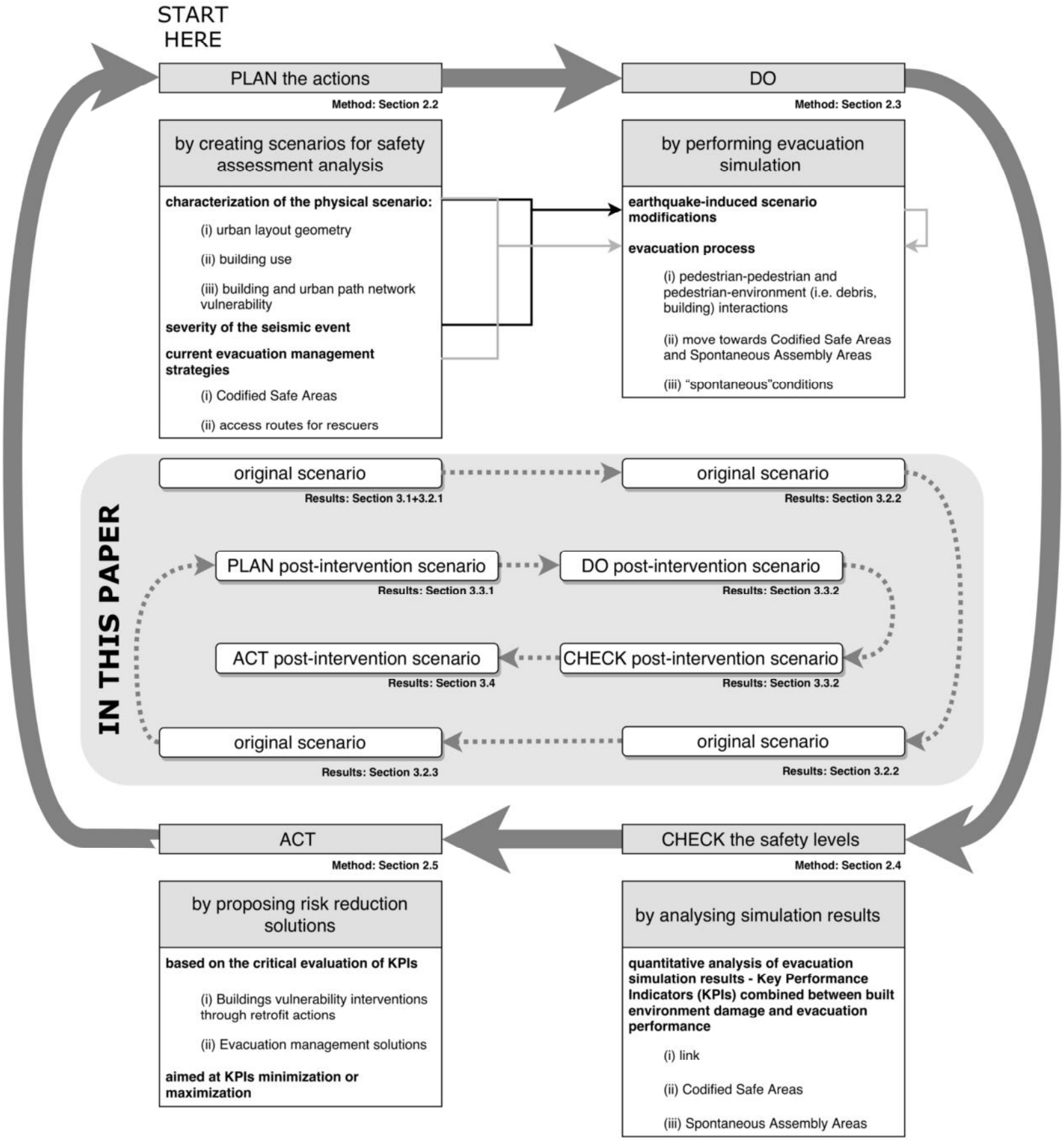
START HERE
PLAN the actions
Method: Section 2.2
by creating scenarios for safety assessment analysis
characterization of the physical scenario:
(i) urban layout geometry
(ii) building use
(iii) building and urban path network vulnerability
severity of the seismic event
current evacuation management strategies
(i) Codified Safe Areas
(ii) access routes for rescuers
DO
Method: Section 2.3
by performing evacuation simulation
earthquake-induced scenario modifications
evacuation process
(i) pedestrian-pedestrian and pedestrian-environment (i.e. debris, building) interactions
(ii) move towards Codified Safe Areas and Spontaneous Assembly Areas
(iii) "spontaneous"conditions
IN THIS PAPER
original scenario
Results: Section 3.1+3.2.1
original scenario
Results: Section 3.2.2
PLAN post-intervention scenario
Results: Section 3.3.1
DO post-intervention scenario
Results: Section 3.3.2
ACT post-intervention scenario
Results: Section 3.4
CHECK post-intervention scenario
Results: Section 3.3.2
original scenario
Results: Section 3.2.3
original scenario
Results: Section 3.2.2
ACT
Method: Section 2.5
by proposing risk reduction solutions
based on the critical evaluation of KPIs
(i) Buildings vulnerability interventions through retrofit actions
(ii) Evacuation management solutions
aimed at KPIs minimization or maximization
CHECK the safety levels
Method: Section 2.4
by analysing simulation results
quantitative analysis of evacuation simulation results - Key Performance Indicators (KPIs) combined between built environment damage and evacuation performance
(i) link
(ii) Codified Safe Areas
(iii) Spontaneous Assembly Areas

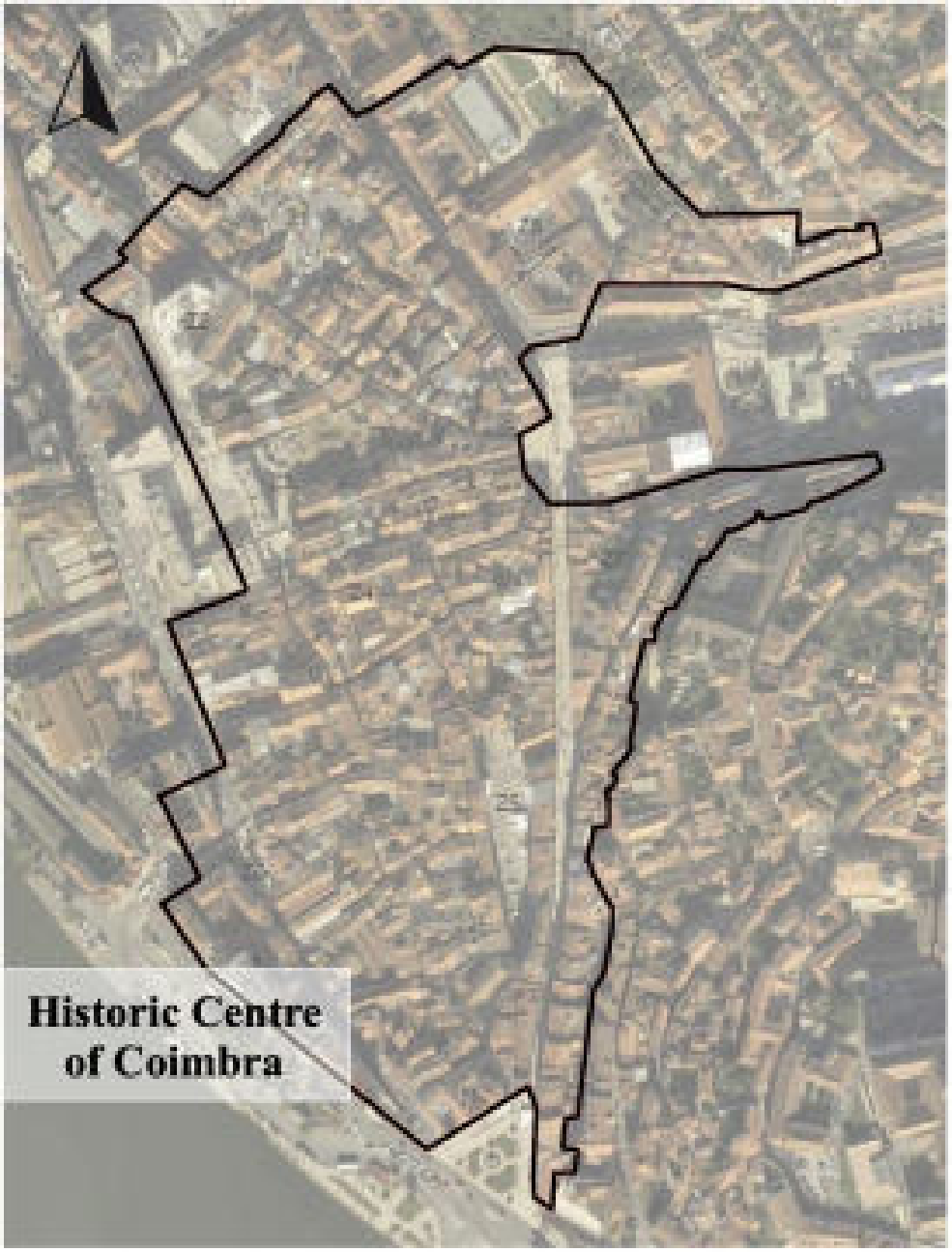
Historic Centre
of Coimbra

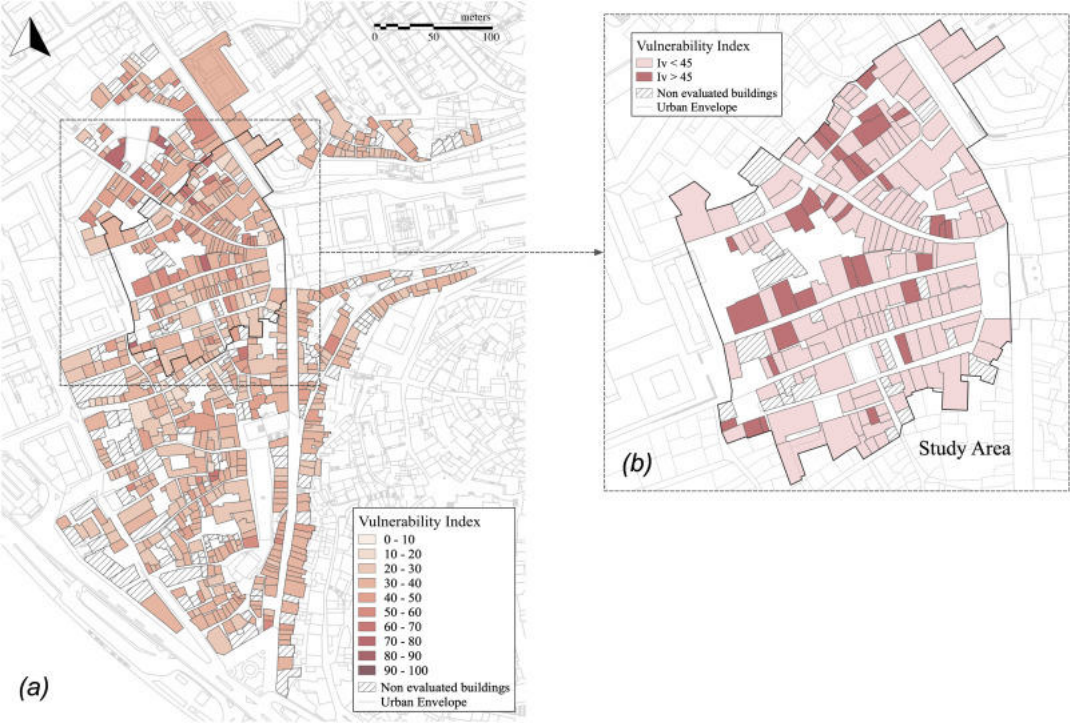
meters
0
50
100
Vulnerability Index
0 - 10
10 - 20
20 - 30
30 - 40
40 - 50
50 - 60
60 - 70
70 - 80
80 - 90
90 - 100
Non evaluated buildings
Urban Envelope
(a)
Vulnerability Index
Iv < 45
Iv > 45
Non evaluated buildings
Urban Envelope
(b)
Study Area


meters
0
20
40
CSA 0
CSA 1
CSA 2
CSA 3
CSA 4
CSA 5
CSA 6
CSA 7
CSA 8
Legend
Nodes
C. Safe Areas
Links(Streets)
Access Point
(a)
(b)
Vulnerability
Links(Streets)
0.0 - 0.1
0.1 - 0.2
0.2 - 0.3
0.3 - 0.4
0.4 - 0.5
0.5 - 0.6
0.6 - 0.7
0.7 - 0.8
0.8 - 0.9
0.9 - 1.0

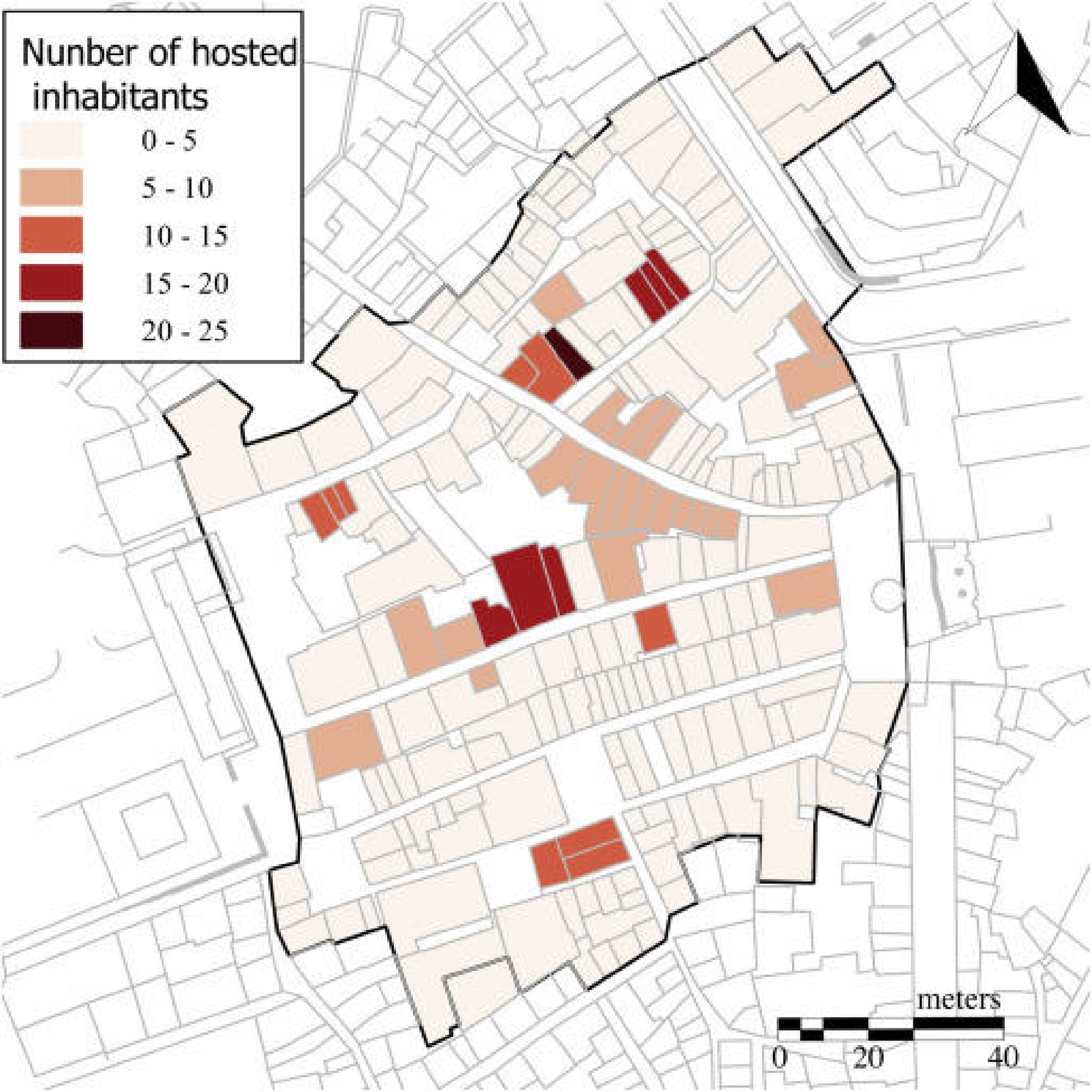
Nunber of hosted inhabitants
0 - 5
5 - 10
10 - 15
15 - 20
20 - 25
meters
0
20
40

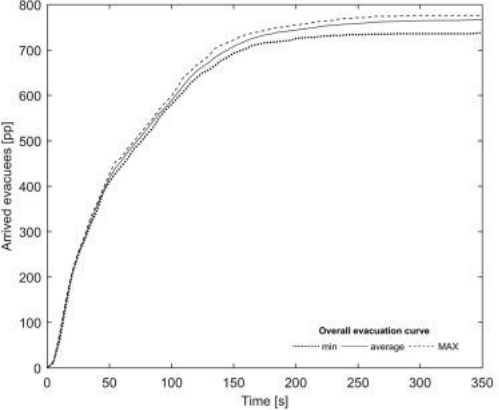
Arrived evacuees [pp]
Time [s]
Overall evacuation curve
min
average
MAX

(a)

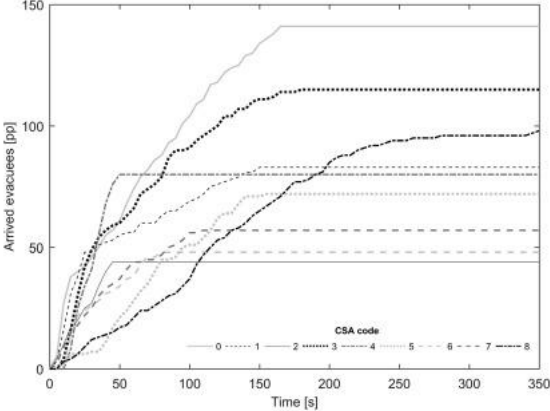
Arrived evacuees [pp]
Time [s]
CSA code
0
1
2
3
4
5
6
7
8

(b)

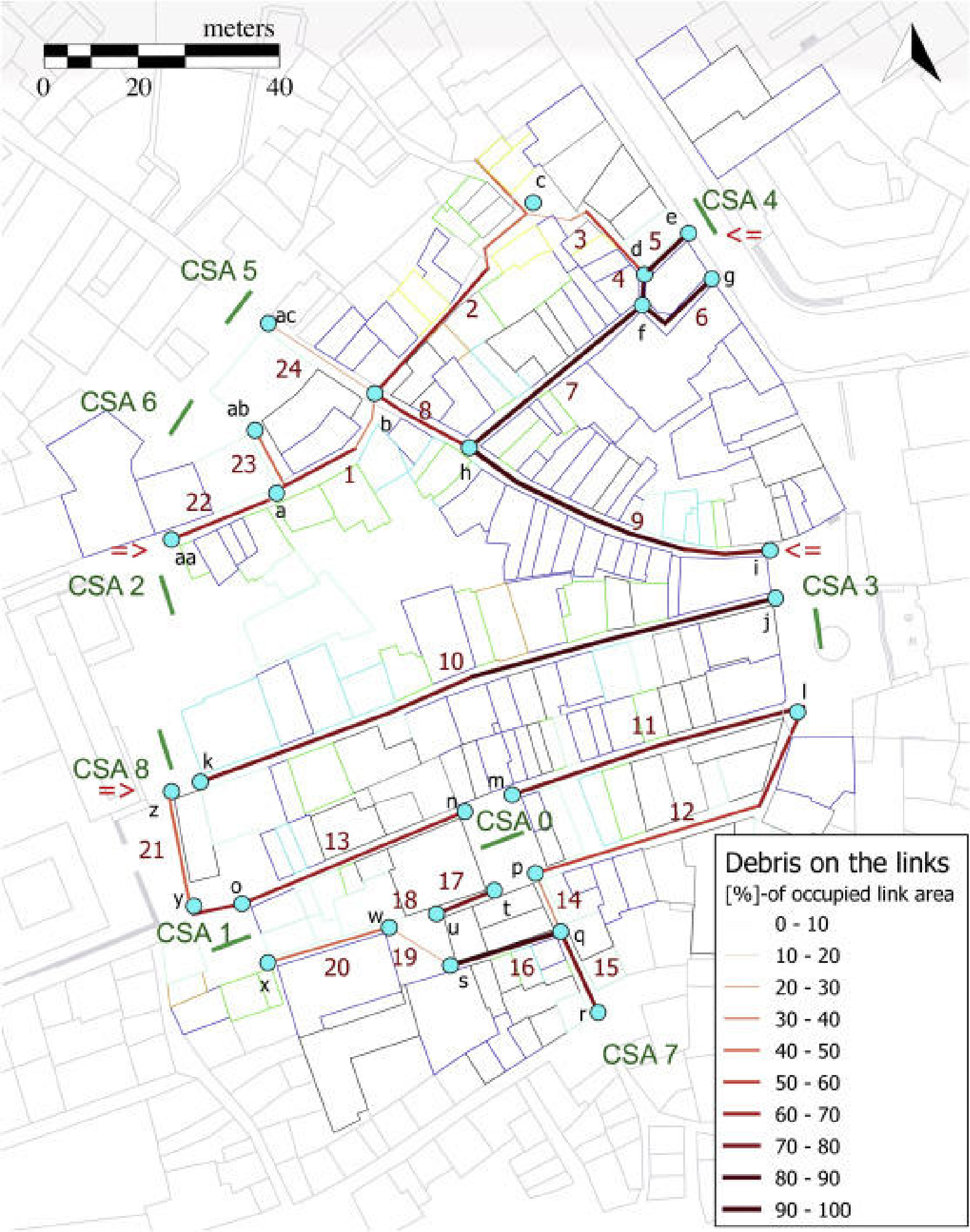
meters
0
20
40
CSA 5
CSA 6
CSA 4
<=
CSA 2
=>
CSA 3
<=
CSA 8
=>
CSA 0
CSA 1
CSA 7
ac
c
e
d
g
f
ab
b
h
i
aa
a
j
k
l
m
n
z
y
o
p
w
u
t
q
x
s
r
24
2
3
5
4
6
7
8
23
1
22
9
10
11
21
13
12
18
17
14
20
19
16
15
Debris on the links
[%]-of occupied link area
0 - 10
10 - 20
20 - 30
30 - 40
40 - 50
50 - 60
60 - 70
70 - 80
80 - 90
90 - 100

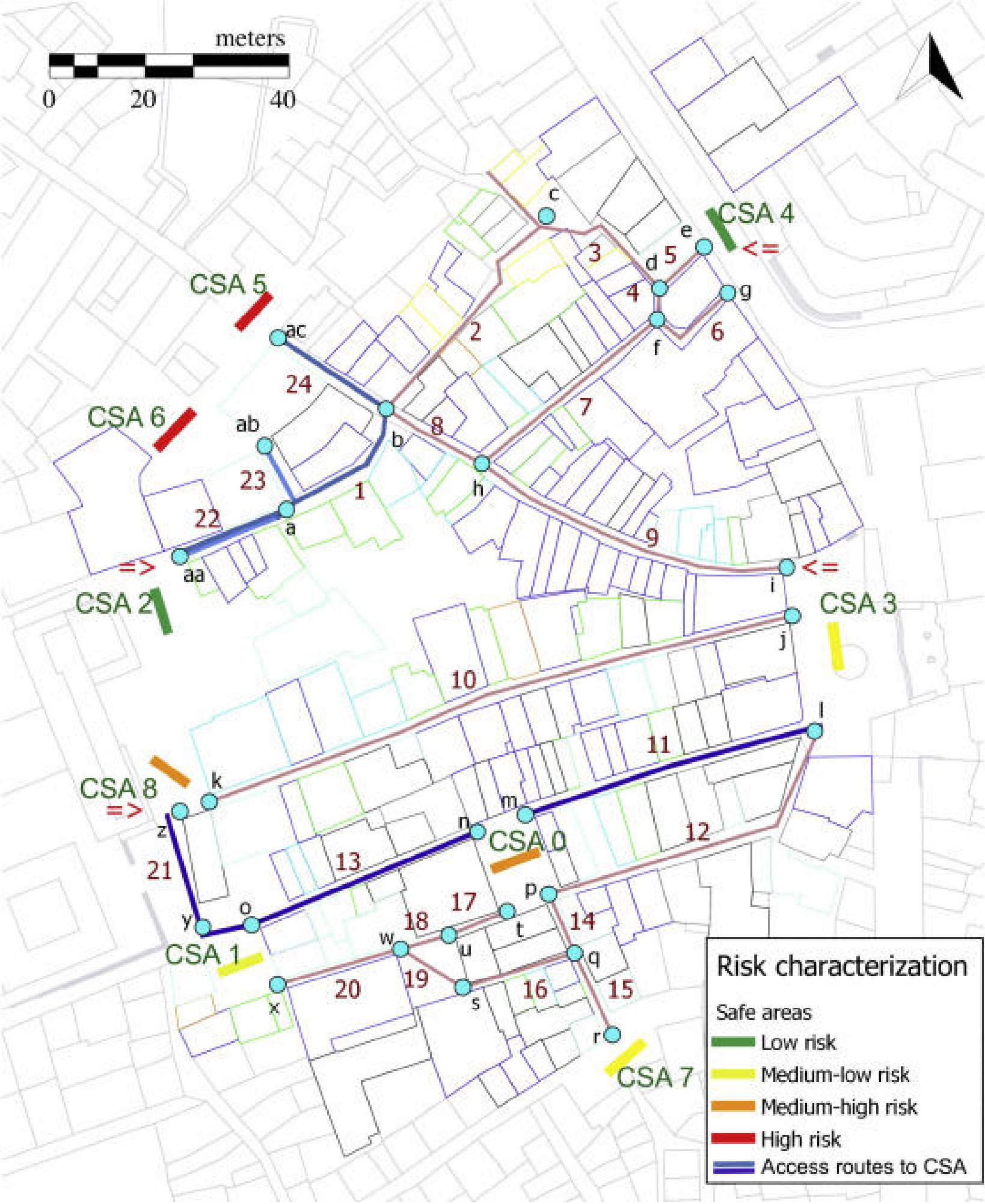
meters
0
20
40
CSA 4
<=
CSA 5
CSA 6
CSA 2
=>
CSA 3
CSA 8
=>
CSA 0
CSA 1
CSA 7
c
e
d
g
f
ac
ab
b
h
a
aa
i
j
k
l
m
n
z
o
y
p
t
w
u
q
x
s
r
1
2
3
4
5
6
7
8
9
10
11
12
13
14
15
16
17
18
19
20
21
22
23
24
Risk characterization
Safe areas
Low risk
Medium-low risk
Medium-high risk
High risk
Access routes to CSA

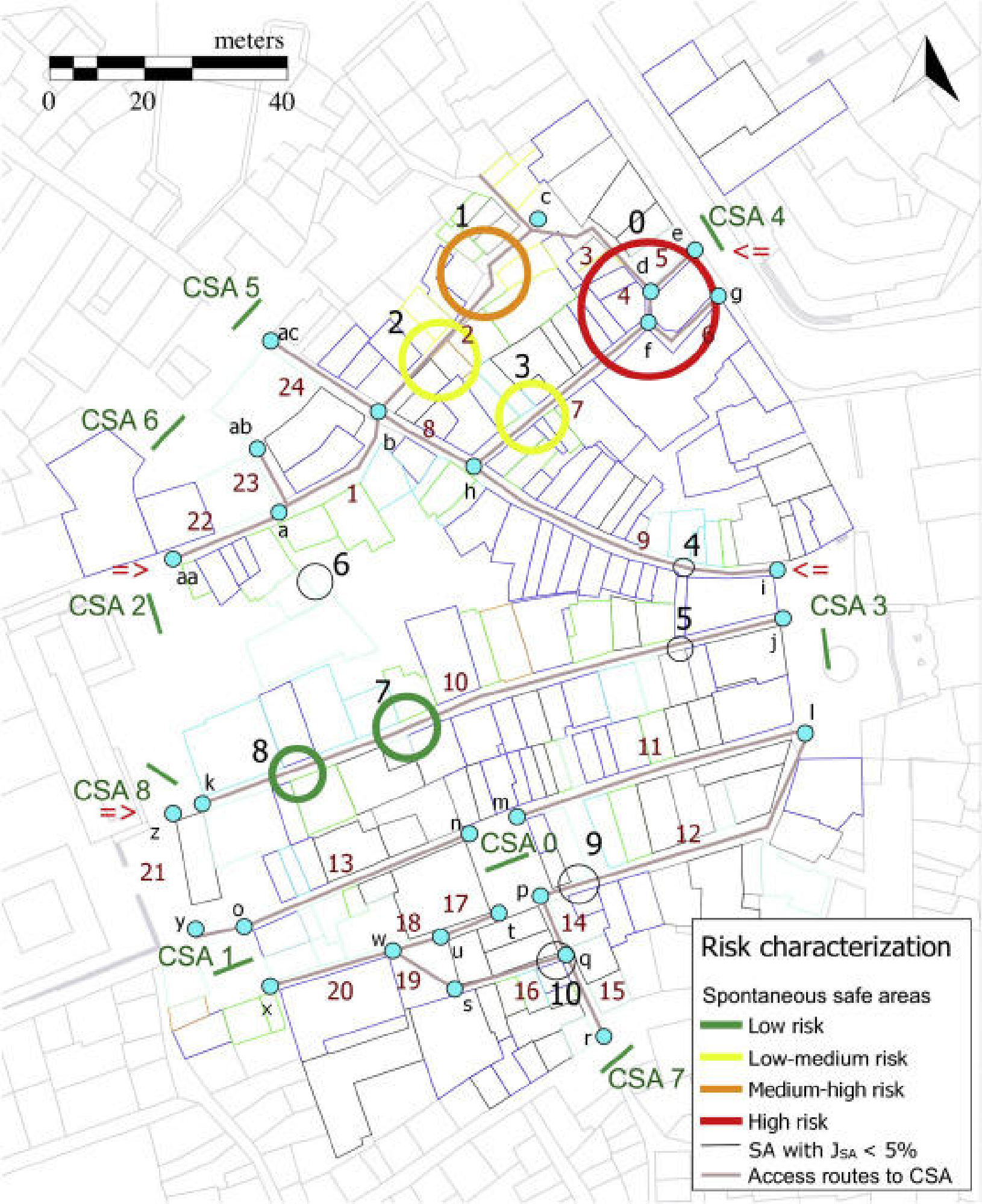
meters
0
20
40
CSA 4
<=
CSA 5
CSA 6
CSA 2
=>
CSA 3
CSA 8
=>
CSA 0
CSA 1
CSA 7
Risk characterization
Spontaneous safe areas
Low risk
Low-medium risk
Medium-high risk
High risk
SA with JSA < 5%
Access routes to CSA

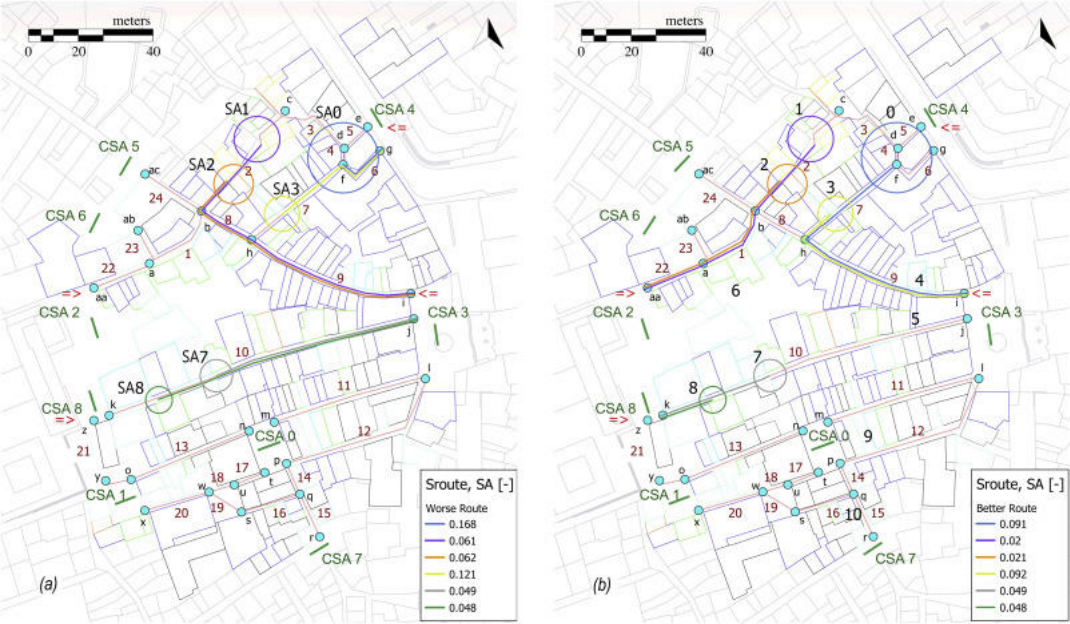
meters
0
20
40
SA1
SA0
SA2
SA3
SA7
SA8
CSA 0
CSA 1
CSA 2
CSA 3
CSA 4
CSA 5
CSA 6
CSA 7
CSA 8
Sroute, SA [-]
Worse Route
0.168
0.061
0.062
0.121
0.049
0.048
(a)
meters
0
20
40
CSA 0
CSA 1
CSA 2
CSA 3
CSA 4
CSA 5
CSA 6
CSA 7
CSA 8
Sroute, SA [-]
Better Route
0.091
0.02
0.021
0.092
0.049
0.048
(b)


meters
0
20
40
Retrofitted Buildings
Links
Study Area
(a)
meters
0
20
40
CSA 0
CSA 1
CSA 2
CSA 3
CSA 4
CSA 5
Legend
Nodes
New C. Safe Areas
Links
(b)

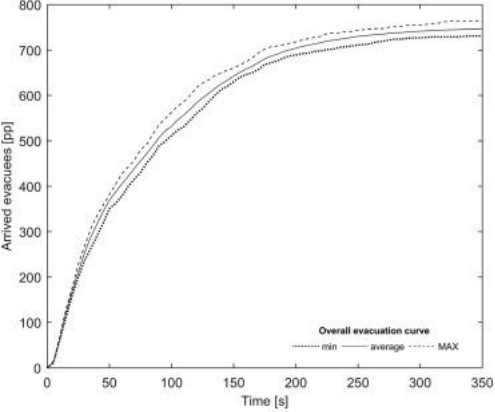
Arrived evacuees [pp]
Time [s]
Overall evacuation curve
min
average
MAX

(a)

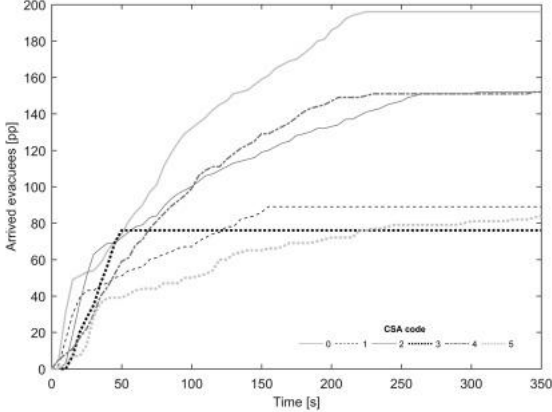
Arrived evacuees [pp]
Time [s]
CSA code
0
1
2
3
4
5

(b)

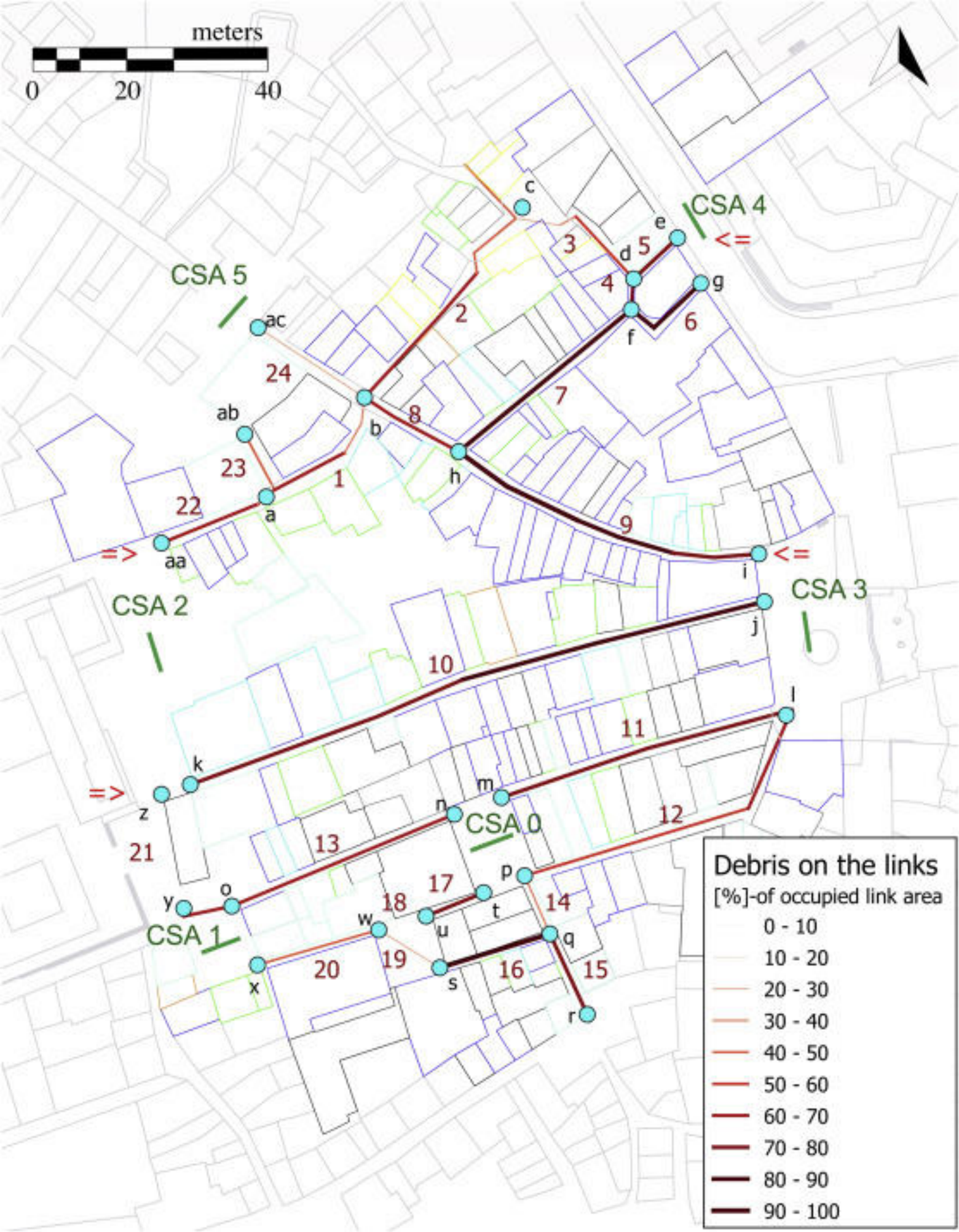
meters
0
20
40
CSA 4
<=
CSA 5
CSA 2
CSA 3
CSA 0
CSA 1
=>
c
e
d
g
f
ac
ab
b
h
a
aa
i
j
k
l
m
n
z
o
y
p
t
u
w
q
x
s
r
1
2
3
4
5
6
7
8
9
10
11
12
13
14
15
16
17
18
19
20
21
22
23
24
Debris on the links
[%]-of occupied link area
0 - 10
10 - 20
20 - 30
30 - 40
40 - 50
50 - 60
60 - 70
70 - 80
80 - 90
90 - 100

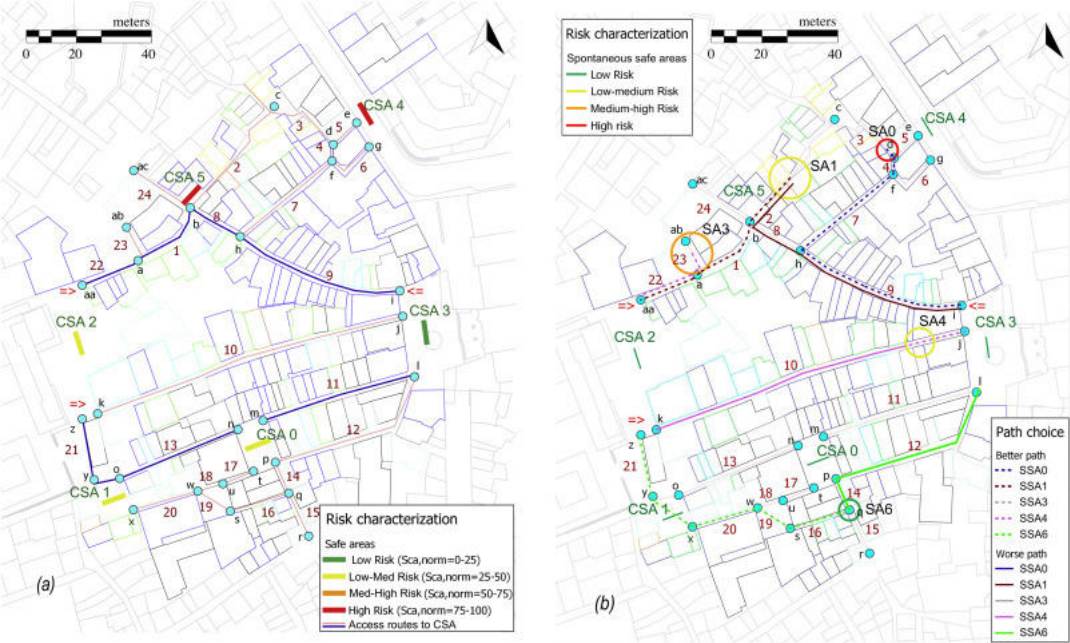
meters
0
20
40
CSA 4
CSA 5
CSA 2
CSA 3
CSA 0
CSA 1
Risk characterization
Safe areas
Low Risk (Sca,norm=0-25)
Low-Med Risk (Sca,norm=25-50)
Med-High Risk (Sca,norm=50-75)
High Risk (Sca,norm=75-100)
Access routes to CSA
(a)
Risk characterization
Spontaneous safe areas
Low Risk
Low-medium Risk
Medium-high Risk
High risk
SA0
SA1
SA3
SA4
SA6
Path choice
Better path
SSA0
SSA1
SSA3
SSA4
SSA6
Worse path
SSA0
SSA1
SSA3
SSA4
SSA6
(b)

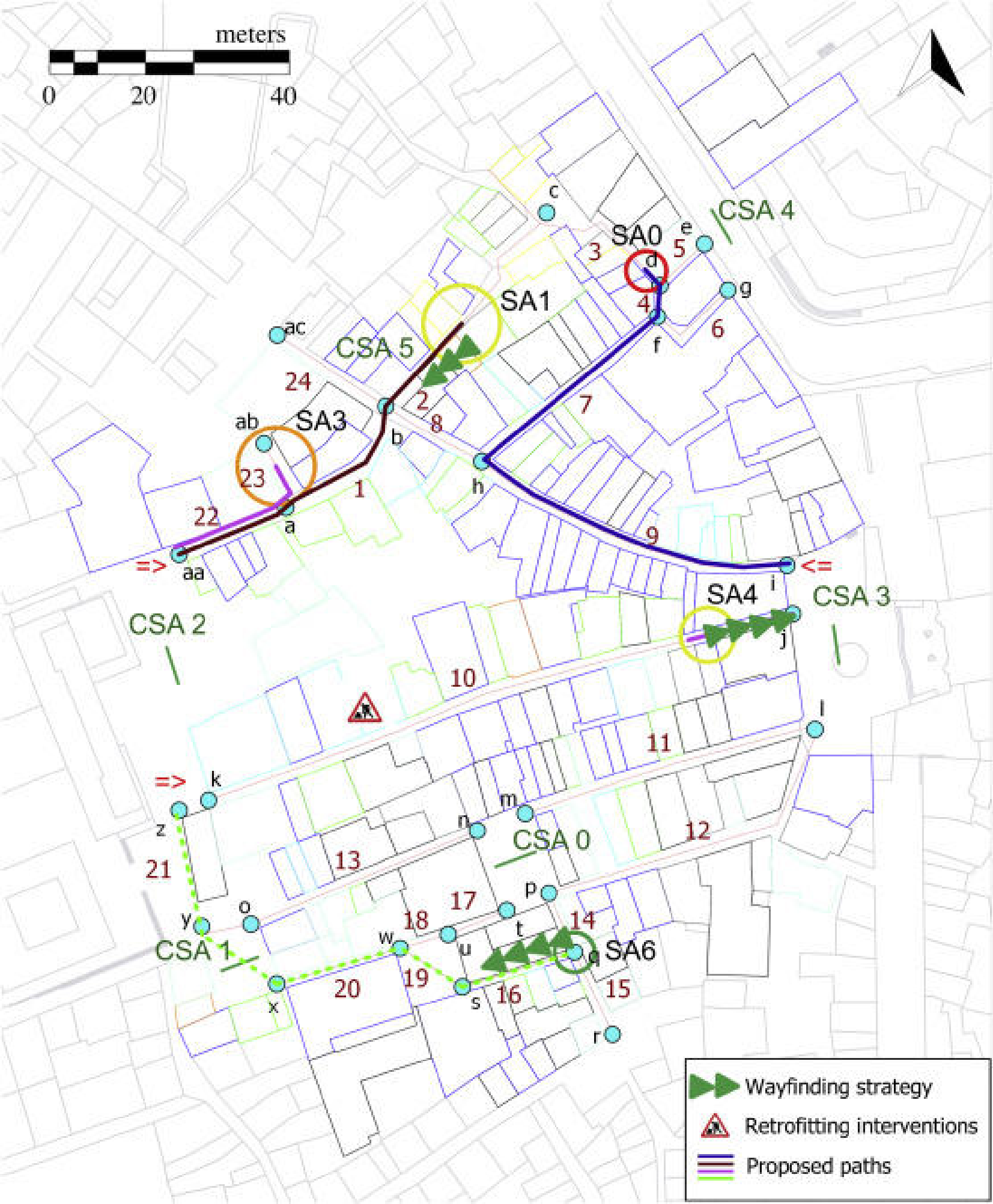
meters
0
20
40
c
SA0
e
CSA 4
3
5
d
g
4
6
f
SA1
ac
CSA 5
24
2
7
8
ab
SA3
b
23
1
h
22
a
=>
aa
9
<=
i
SA4
CSA 3
CSA 2
j
10
l
11
=>
k
m
z
n
CSA 0
12
21
13
p
17
o
y
18
14
w
t
u
CSA 1
SA6
q
20
19
16
15
x
s
r
Wayfinding strategy
Retrofitting interventions
Proposed paths

KPI (symbol) [unit of measurement] – KPI domain	Computation procedure	Interpretation
Link vulnerability V_{link} [−] – from 0 to 100	See Appendix C	The higher V_{link}, the higher the possibility of debris generation.
Number of evacuees using a certain *link* to reach a certain CSA ($N_{av,link}$) [pp] - ≥0 pp	Simulation output by tracking pedestrians' path; it is calculated as average value for the performed simulations. It can be associated to [%] which is the related percent standard deviation.	The higher this value, the higher the importance of the *link* in respect to the considered *CSA*.
Link surface occupied by debris ($A_{debris,link}$) [m^2] - ≥0 m^2	Calculated according to the debris generation algorithm (see Appendix D)	Interferences with debris.
Effective CSA surface ($A_{eff,link}$) [m^2] - ≥0 m^2	Difference between the *link* area (without considering courtyards and other not accessible areas) and $A_{debris,link}$	
Occupancy index for the given *link* (O_{link}) [−] – from 0 to 1	$O_{link} = \min\left(\frac{A_{ruins,link}+N_{av,link}\cdot(1+\%\sigma_{Nav,link})\cdot dA_{ped,D}}{W_{link}\cdot L_{link}};1\right)$ (1) where $A_{debris,link}$ [m^2] is the area of debris along the considered link (according to the debris generation algorithm in Appendix D) and is $dA_{ped,D}$ [m^2] the average moving pedestrian's area (fixed at 0.25 m^2) in Level of Service D conditions (Klüpfel and Meyer-König 2014)	Describes the crowding conditions (including debris influence) by ideally considering all the pedestrians moving together.
Safety index for rescuers' access to the link of a defined access route ($S_{link,SAA}$) [−] – from 0 to 1	$S_{link,SAA} = \left(\frac{A_{debris,link}}{A_{eff,link}+A_{debris,link}}\right)\cdot\left(\min\left(\frac{N_{av,link}}{A_{eff,link}/dA_{ped,D}};1\right)\right)\cdot\left(1-\frac{pos_{link}}{n_{link,route}}\right)$ (2) where pos_{link} is the position of the considered link inside the rescuers' path can be evaluated by considering the number $n_{link,route}$ of links composing the access route. The overall value is 1.0 for the link closer to the SAA.	The terms respectively consider: the debris influence, the evacuees' density conditions ($A_{eff,link}/dA_{ped,F}$ is the maximum reachable number of people along the link itself); the position of the link within the access route. The value can be normalized within the area $S_{link,SAA,norm}$ to define a priority list for interventions.

Table 1

KPI (symbol) [unit of measurement] – KPI domain	Description and computation procedure	Interpretation
Percentage of evacuees arrived at CSA (J_{CSA}) [%] – from 0% to 100%	Ratio between the total of $N_{av,link}$ and the total number of evacuees involved in the simulation	The higher this value, the higher the importance of the CA in the evacuation process, the higher the possibility to reach overcrowding conditions. Risk-reduction proposals should maximize the number of evacuees arrived in a CSA, by minimizing the number of CSA to focus rescuers' actions.
Difference-in-path ratio (T) [−] – 0 to 2	Length ratio between the effective evacuation path and the ideal one; calculated as average value for all the evacuees arrived to the CSA. Values higher than 2 are arbitrarily considered equal to 2.	The higher T, the more winding is the path to reach CA, the higher the number of times in which the pedestrians change its direction (i.e. for pedestrians' and debris avoidance, for coming-and-going behaviors on the links)
Interference between evacuees moving towards the CSA on the link (F_{link}) [−] – from 0 to 1	$F_{link} = \frac{N_{av,link}}{\sum_{link=1}^{n} N_{av,link}}$ (3)	it expresses the interferences between evacuees by considering how many people arrive in a certain CSA by using the considered link
Safety index of a link to a CSA ($S_{link,CSA}$) [−] – from 0 to 1	Applied to a link that is placed along a rescuers' access route by multiplying O_{link} and F_{link}	It describes the possible interferences to the rescuers' access connected to evacuees and path debris interaction. The higher this value, the more sensible interferences are noticed in the link. The value can be normalized within the area $S_{link,CSA,norm}$ to define a priority list for interventions.
CSA surface occupied by debris (A_{debris}) [m^2] - ≥0 m^2	Calculated according to the debris generation algorithm (see Appendix D)	Interferences with debris.
Effective CSA surface (A_{eff}) [m^2] - ≥0 m^2	Difference between the CSA area (without considering courtyards and other not accessible areas) and A_{debris}	
Evacuation curve at the CSA ([pp] versus [s])	Number of arrived people against the simulation time, through a graphical representation	Risk reduction proposals should minimize the evacuation time by maximizing evacuees' flows towards few selected CSA (i.e., increasing the curve slope).
Occupancy in the CSA (LOS_{CSA}) [m^2/pp] – >0 m^2/pp	Ratio between A_{eff} and the total of $N_{av,link}$; values < 0.18 m^2/pp can be considered as unacceptable since they are connected to evacuees' densities > 5.3 pp/m^2 (physical contacts)	Risk reduction proposals should allow actions for areas management (i.e.: localization, evacuees' wayfinding support) aimed at limit LOS_{CSA}≥0.3 m^2/pp (no physical interactions between individuals)

KPI (symbol) [unit of measurement] – KPI domain	Description and computation procedure	Interpretation
CSA safety index S_{CSA} [−] – from 0 to 1.73	$S_{CSA} = \sqrt{J_{CSA}^2 + (T-1)^2 + \left(\sum_{link=1}^{n} S_{link,CSA}\right)^2}$ (4)	It describes the safety of CSA due to the number of arrived people and their interference in motion along the used *links*. The value can be normalized within the area S_{CSA} to define a priority list for interventions.

Table 2

KPI (symbol) [unit of measurement] – KPI domain	Description and computation procedure	Interpretation
Percentage of evacuees spontaneously gathering in a SAA (J_{SAA}) [%] – from 0% to 100%	Ratio between the total of simulated individuals gathering near a same urban fabric area and the total number of evacuees not arrived to a safe area. Since an error in path choice is introduced (10%) and simulation output differences could exist and be ≤ 10%, it is proposed that SAA are considered as effective if they collect at least the 5% of not arrived people to CSAs	The higher this value, the higher the importance of the SAA in the evacuation process. Hence, significant SAA could be turned into CSA and the number of evacuees arrived in a CSA should be maximized.
SAA surface occupied by debris ($A_{debris,SAA}$) [m^2] - ≥0 m^2	Calculated according to the debris generation algorithm (see Appendix D)	Interference with debris by including data on each facing building
Effective SAA surface ($A_{eff,SAA}$) [m^2] - ≥0 m^2	Difference between the SAA area (without considering courtyards and other not accessible areas) and $A_{debris,SAA}$	
Debris occupancy ($R_{b,SAA}$) [−] – from 0 to 1	$$R_{b,SAA} = \sum_b \left(\frac{W_{SAA}/2}{W_{center,b}} \cdot \frac{d_{debris,b}}{W_{center,b}} \right) \quad (5)$$ where b is the considered building facing the SAA, W_{SAA} [m] is the SAA width, $W_{center,b}$ [m] is distance from the geometrical SAA centre and the interfering building side, and $d_{debris,b}$ [m] is the debris average depth for the considered building	
SAA intrinsic safety ($S_{area,SAA}$) [−] – from 0 to 1	$$S_{area,SAA} = R_{b,SAA} \cdot \left(\min \left(\frac{N_{av,SAA}}{A_{eff,SAA}/dA_{ped,D}}; 1 \right) \right) \cdot \left(\frac{1}{n_{acc}} \right) \quad (6)$$ where n_{acc} [−] is the number of possible accesses to SAA (4 for a four roads crossroad and wide squares; 2 along a street; 1 for blind alley)	Data related to the SAA itself affect the possibility to wait in that SAA in safe conditions considering geometry versus damages and hosted individuals' density, and the possibility of access to the area. The higher the value, the more "dangerous" conditions can be noticed for the hosted evacuating pedestrians.
Safety index for rescuers' access route $S_{route,SAA}$ [−] – from 0 to 1	$$S_{route,SAA} = \left(\sum_{n_{link}=1}^{n_{link}} S_{link,SAA} \right) / n_{link} \quad (7)$$ where n_{link} represents the number of links composing the rescuers' access route.	The index considers all the number of links that compose the rescuers' access path. The higher the value, the more "dangerous" conditions for rescuers' access.
SAA safety index S_{SAA} [−] – from 0 to 1.73	$$S_{SAA} = \sqrt{J_{SA}^2 + S_{path,SAA}^2 + S_{area,SAA}^2} \quad (8)$$	It describes the safety of SAA due to the number of arrived people, the access route conditions and the SAA conditions for evacuees' staying. The value can be normalized within the area S_{SAA} to define a priority list for interventions.

Table 3

CSA	0	1	2	3	4	5	6	7	8
$A_{eff,CSA}$ [m^2]	303	237	550	545	265	250	250	300	380
Np [pp]	141 + 20[a]	83	44	115 + 12[a]	80	72	48	57	98
J_{CSA} [%]	18%	11%	6%	15%	10%	9%	6%	7%	13%
LOS_{CSA}	2.2	2.9	12.5	4.3	3.3	3.5	5.2	5.3	3.9

a Refers to evacuees who, although have not reached the CSA, have stopped really close to it and therefore are not included in the J_{CSA} calculation.

Table 4

CSA	0	1	2	3	4	5	6	7	8
T [−]	1.254	1.157	1.059	1.265	1.034	1.437	1.323	1.227	1.402
$\Sigma S_{link,CSA}$	0.036	0.012	0.000	0.000	0.000	0.265	0.317	0.000	0.000
S_{CSA} [−]	0.369	0.219	0.083	0.314	0.110	0.630	0.649	0.261	0.408
$S_{CSA\ (Norm)}$	57%	34%	13%	48%	17%	97%	100%	40%	63%

Table 5

SAA	0	1	2	3	7	8
$A_{eff,SAA}$ [m^2]	18	39	33	23	63	63
$S_{area,SAA}$ [−]	0.345	0.075	0.118	0.193	0.056	0.046
$S_{route,SAA}$ [−]	0.091	0.044	0.044	0.083	0.042	0.042
J_{SA} [%]	19%	10%	10%	8%	7%	6%
S_{SAA} [−]	0.406	0.137	0.159	0.225	0.103	0.088
$S_{SAA\ (Norm)}$	100%	34%	39%	56%	25%	22%

Table 6

Link	Building code	Original I_{vf}	Post-intervention I_{vf}	I_{vf} Reduction [%]
Link 4	6.1	35.78	26.13	26.97
	7.7	32.61	23.04	29.35
Link 6	6.1	35.78	26.13	26.97
Link 7	7.1	50.00	42.17	15.66
	7.2	48.48	41.30	14.81
	7.3	59.57	52.61	11.68
	7.5	34.5	24.50	28.99
	7.7	32.61	23.04	29.35
Link 9	9.1	42.17	23.91	43.30
	9.2	45.00	33.48	25.60
	9.3	33.61	26.02	22.58
	9.4	56.52	49.13	13.08
	9.5	50.07	38.65	22.81
	9.7	59.13	41.74	29.41
	9.9	50.07	38.65	22.81
Link 10	10.1	56.96	34.35	39.69
	10.2	46.37	38.65	16.65
	10.3	59.20	37.44	36.76
	10.4	54.13	32.17	40.57
	10.5	45.72	23.09	49.50
	10.7	74.78	53.04	29.07
	10.9	43.26	23.91	44.73
	10.11	49.13	26.52	46.02

Table 7

Link	Total Area [m^2]	Original condition			Post-intervention conditions		
		V_{link}	A_{debris}[m^2]	Free Area [%]	V_{link}	A_{debris} [m^2]	Free Area [%]
Link 4	14.75	0.53	11.87	20	0.38	10.78	27
Link 6	55.06	0.57	45.21	18	0.49	43.25	21
Link 7	150.76	0.71	128.10	15	0.65	122.90	18
Link 9	240.72	0.66	210.93	12	0.60	202.73	16
Link 10	441.33	0.69	342.04	22	0.59	325.27	26

Table 8

CSA	0	1	2	3	4	5
$A_{eff,CSA}$ [m^2]	303	237	930	545	265	167
Np [pp]	196	89	152 + 5[a]	76 + 11[a]	152	84 + 17[a]
LOS_{CSA}	1.546	2.663	5.931	6.279	1.743	1.653
$J_{CSA,pi}$ [%]	26%	12%	20%	10%	20%	11%
Original CSA	0–7	1	2–8	3	4	5–6
$J_{CSA,0}$ [%]	18% + 7%	11%	6% + 13%	15%	10%	9% + 6%
dJ_{CSA} [%]	5%	8%	7%	−32%	104%	−25%

a

Refers to people not arrived in the CSA but stopped really close to it and that are not included in the J_{CSA} calculation.

Table 9

CSA	0	1	2	3	4	5
J_{CSA} [%]	26%	12%	20%	10%	20%	11%
T [−]	1.329	1.181	1.273	1.023	1.578	1.248
$\Sigma S_{link,CSA,pi}$	0.001	0	0	0	0	0.170
S_{CSA} [−]	0.421	0.216	0.341	0.104	0.613	0.494
$S_{CSA,Norm}$	49%	35%	50%	17%	100%	81%
Original CSA	0	1	8	3	4	5
T_o [−]	1.254	1.157	1.402	1.265	1.034	1.437
dT [%]	6%	2%	−9%	−19%	53%	−13%
$\Sigma S_{link,CSA,o}$	0.020	0.000	0.000	0.000	0.000	0.288
$S_{CSA,o}$ [−]	0.369	0.219	0.408	0.314	0.110	0.630
dS_{CSA} [%]	14%	−1%	−16%	−67%	457%	−22%

Table 10

SAA	0	1	3	4	6
$A_{eff,SAA}$ [m^2]	21	33	54	45	122
$S_{area,SAA}$ [−]	0.077	0.157	0.013	0.150	0.021
$S_{route,SAA}$ [−]	0.110	0.042	0.024	0.020	0.003
J_{SA} [%]	5%	15%	9%	13%	20%
S_{SAA} [−]	0.144	0.221	0.094	0.203	0.197
$S_{SAA,norm}$ [−]	65%	100%	43%	90%	89%
Original SAA	0	2	–	–	–
$A_{eff,SAA,o}$ [m^2]	18	33	–	–	–
$d\,A_{eff,SAA}$ [%]	33%	0%	–	–	–
$S_{area,SAA,o}$ [−]	0.345	0.118	–	–	–
$dS_{area,SAA}$ [−]	−78%	33%	–	–	–
$S_{route,SAA,o}$ [−]	0.091	0.043			
$dS_{route,SAA}$ [%]	20%	−2%			
$J_{SAA,o}$ [%]	19%	10%	–	–	–
dJ_{SAA} [%]	−73%	−55%	–	–	–
$S_{SAA,o}$ [−]	0.345	0.118	–	–	–
dS_{SA} [%]	−61%	41%	–	–	–

Table 11

Symbol	Measure	Description
I^*_{vf}	–	Façade walls vulnerability index (Tiago M. [18]).
I_{vf}	–	Normalized façade walls vulnerability index
C_{vi}	–	Assigned score for each class for façade walls vulnerability index estimation
p_{vi}	–	Assigned weighting factor to vulnerability influencing parameters for façade walls vulnerability index estimation
V_{link}	–	Seismic vulnerability of the link [15]
i	–	Incidence of the building in the link, as ratio between building and link lengths
EPES	–	Earthquake Pedestrians' Evacuation Simulator [44]
CSA	–	Codified safe areas
SAA	–	Spontaneous safe areas
I_{EMS-98}	–	Earthquake intensity according to the European Macroseismic Scale [66]
S_{CSA}	–	Safety levels evaluation of codified safe area CSA
$J_{p,s}$	–	Describes the percentage of pedestrians joining the considered safe area
T	–	Pedestrians' difference-in-path ratio (indicator of the link tortuosity)
$S_{link,CSA}$	–	Safety index referred to a link arriving in a codified safe area
O_{link}	–	Link occupancy index which includes pedestrian's area and ruins presence
A_{ruins}	m^2	Link area occupied by ruins and debris presence
$N_{av,link}$	–	Average number of pedestrians using the path
$\%\sigma_{N,sim}$	–	Correction factor on pedestrian's link usage
$dA_{ped,E-F}$	m^2	Average moving pedestrian's area (fixed at 1 m^2)
W_{link}	m	Average width of the link
L_{link}	m	Total length of the link
F_{link}	–	Interference between the evacuating pedestrians evaluating through the normalized flow along the link
LOS	$m^2/person$	Level of Service
A_{eff}	m^2	Link effective area removing the inaccessible area and the area occupied by ruins
N_p	–	Number of gathered pedestrians in a CA
$S_{area,SA}$		Intrinsic safety level of a spontaneous safe area
$A_{eff,SA}$	m^2	Effective area of spontaneous assembly point removing the inaccessible area and the area occupied by ruins
W_{SA}	m	Width of the SAA from one side to another
$W_{center,b}$	m	Distance from the geometrical SAA centre and the interfering building side
$d_{ruins,b}$	m	Average depth of ruins along the link
$N_{av,SA}$	–	Average simulated number of pedestrians in SAA
n_{exits}	–	The number of possible accesses to the area
$S_{path,SAA}$	–	Represents the sum of all $S_{links,\ SA}$ normalized for the number of links that compose the rescuers' access path
$S_{link,SAA}$	–	Safety level of a link employed to reach a spontaneous safe area by rescuers
n_{link}	–	Number of links that compose the rescuers' access path
$A_{plan,tot}$	m^2	Link total area
$A_{plan,inc}$	m^2	Link inaccessible areas (e.g.: private courtyards, fenced areas)
$A_{eff,link}$	m^2	Effective area of links removing the inaccessible area and the area occupied by ruins
pos_{link}	–	Assumed positions of the considered link inside the rescuers' path
$n_{link,path}$	–	Total number of links composing the path

Table A1

Acronym	Description
ABM	Agent-Based Model
CSA	Codified Safe Areas, which are the assembly areas actually included in the emergency plan
EPES	Earthquake Pedestrians' Evacuation Simulator [44]
KPI	Key Performance Indicators
PDCA	Plan-Do-Check-Act
SAA	Spontaneous Assembly Area, which are areas in the urban fabric where people can gather and end the evacuation process because of social phenomena and the impossibility to reach a CSA
SFM	Social Force Model, which represents the human motion in the evacuation process according to Ref. [55]

Table A2

Parameters	Class, C_{vi}				Weight p_i	Relative Weight
	A	B	C	D		
Group 1. Façade geometry, openings and interaction						
P1. Geometry of the façade	0	5	20	50	0.50	16.7/100
P2. Maximum slenderness	0	5	20	50	0.50	
P3. Area of openings	0	5	20	50	0.50	
P4. Misalignment of openings	0	5	20	50	0.50	
P5. Interaction between contiguous facades	0	5	20	50	0.25	
Group 2. Masonry materials and conservation						
P6. Quality of materials	0	5	20	50	2.00	31.5/100
P7. State of conservation	0	5	20	50	2.00	
P8. Replacement of original flooring system	0	5	20	50	0.25	
Group 3. Connection efficiency. to other structural elements						
P9. Connection to orthogonal walls	0	5	20	50	2.00	33.3/100
P10. Connection to horizontal diaphragms	0	5	20	50	0.50	
P11. Impulsive nature of the roofing system	0	5	20	50	2.00	
Group 4. Elements connected to the façade wall						
P12. Elements connected to the façade	0	5	20	50	0.50	18.5/100
P13. Improving elements		5	20	50	−2.00	

Table B1